

Solar Flares

- *Hinode* Perspective -

SOT


EIS

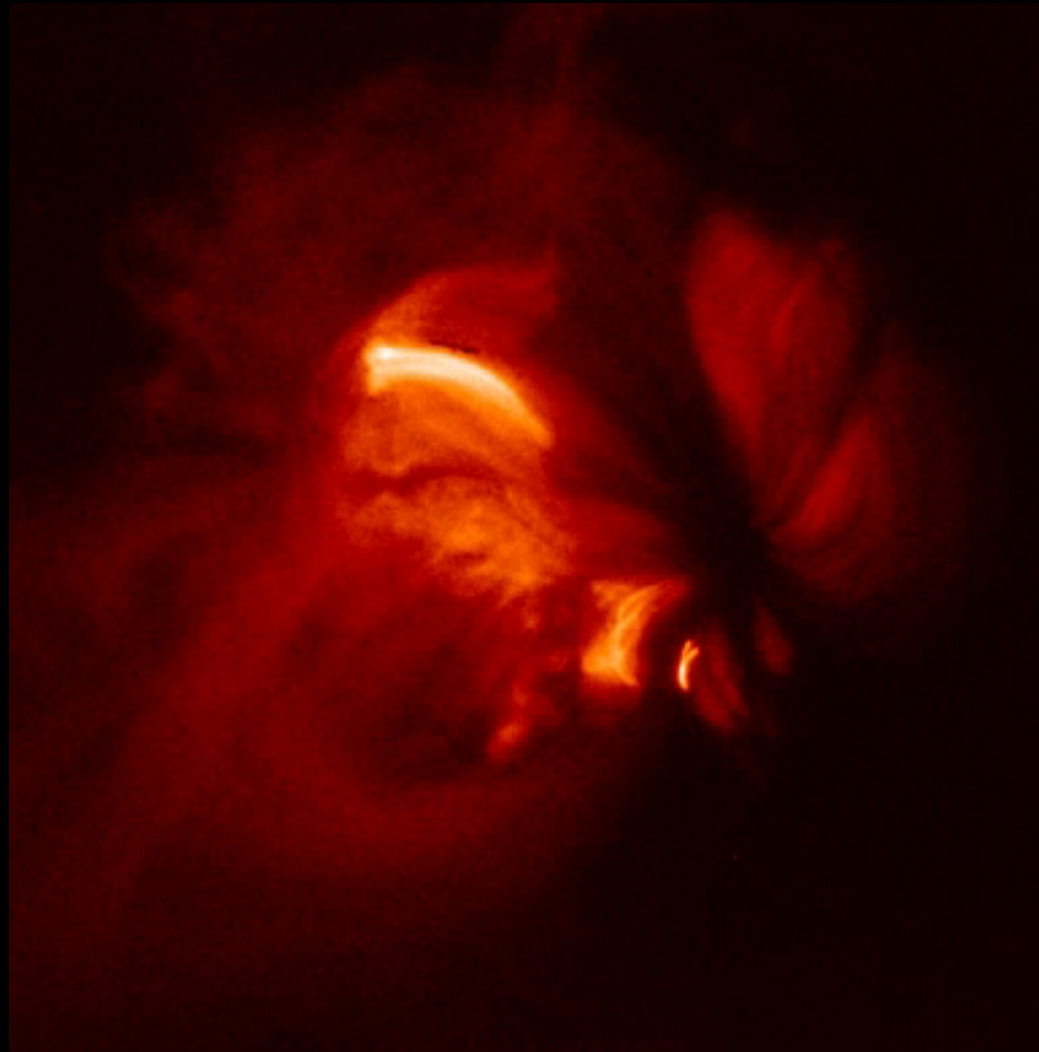
XRT

Hirohisa Hara
NAOJ

Coupling and Dynamics of the Solar Atmosphere
2014 Nov 10 – 14 @IUCAA, Pune, India

Solar Flare Research by *Hinode*

- Solar flares:
 - explosive events on the Sun that produce $>10\text{MK}$ plasmas and high-energy particles by heating and particle-acceleration processes.
 - Research Topics
 - Energy storage and trigger processes
 - Particle acceleration and chromospheric evaporation
 - Magnetic reconnection
 - Unique Approach by *Hinode* (SOT + XRT +EIS)
 - High-resolution; especially SOT sub-arcsec imaging
 - Photo. vector B field (imaging & spectro-polarimetry)
 - High-cadence X-ray imaging
 - EUV scanning spectroscopy
- Limited capability
- 

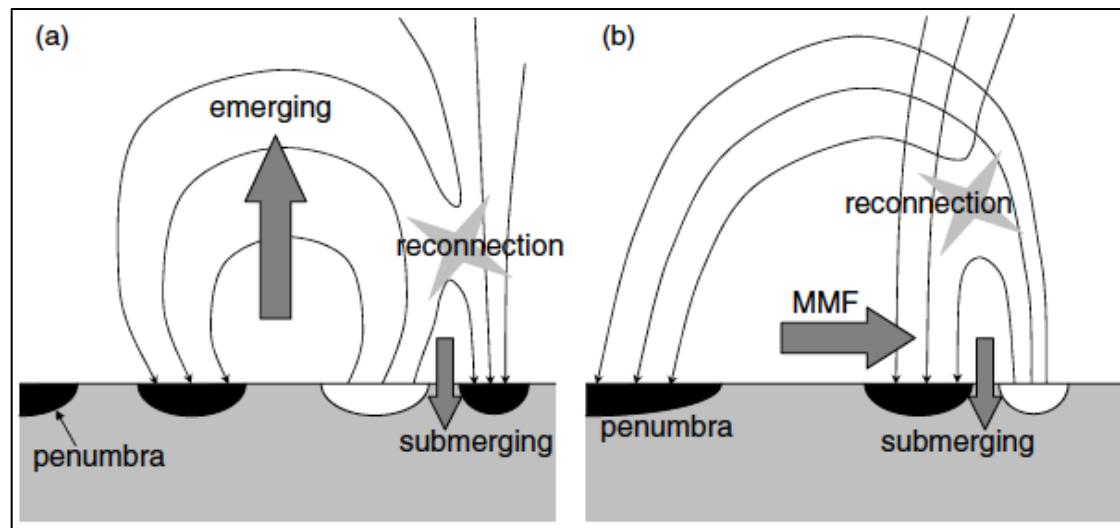
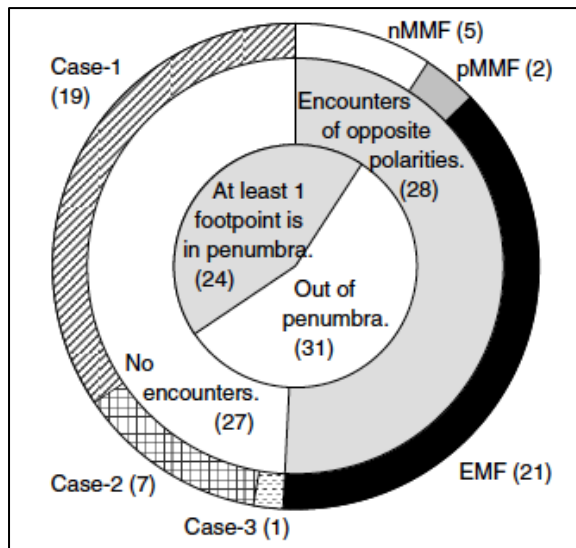
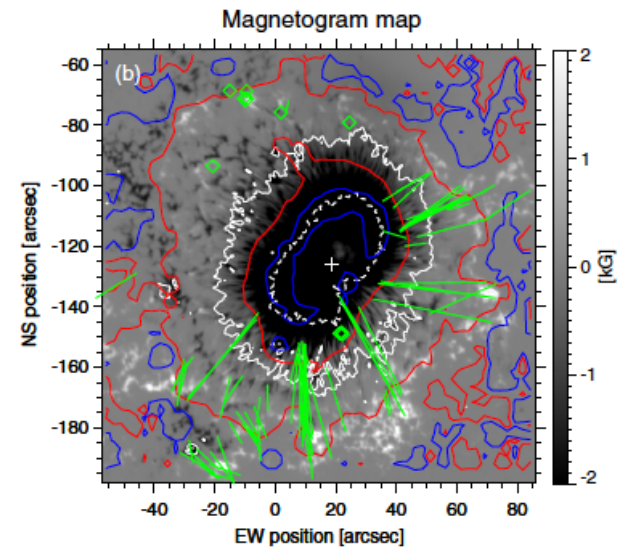
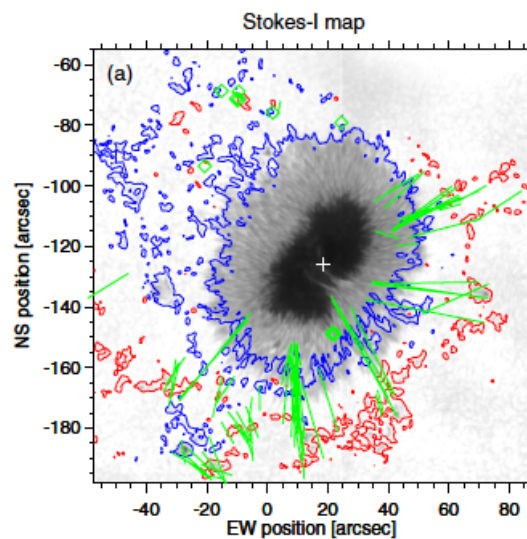
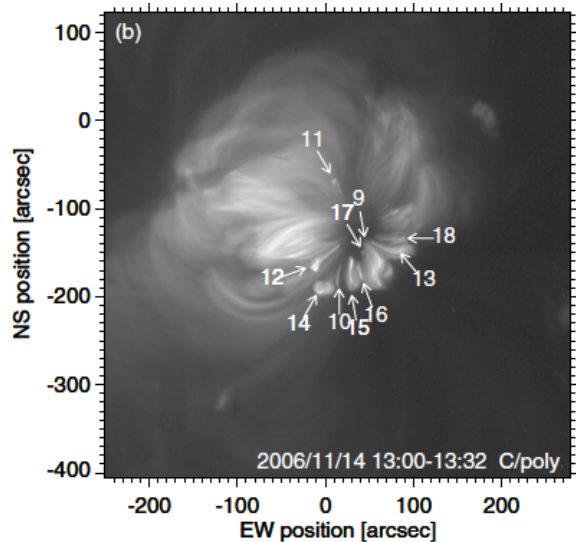


Microflares

Magnetic Connectivity & Morphology

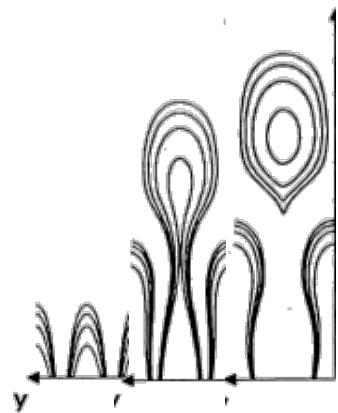
XRT + SOT

Kano et al. (2010)

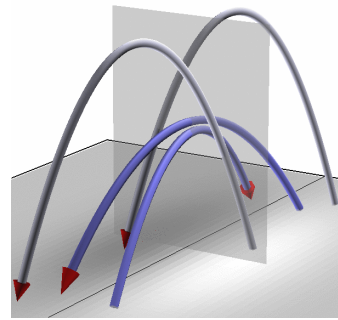


Onset Problem of Solar Eruptions

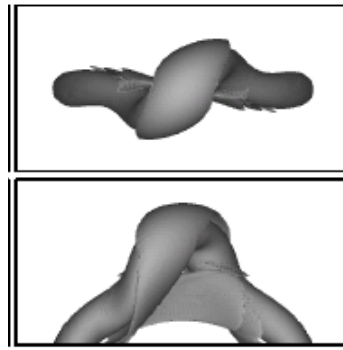
- Various models have been proposed to explain the onset of solar eruptions.



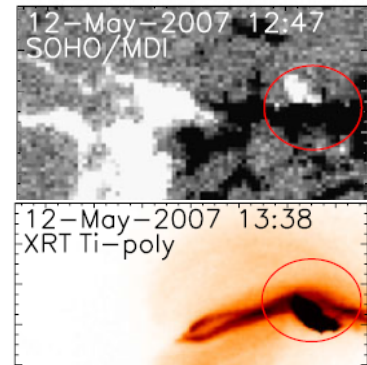
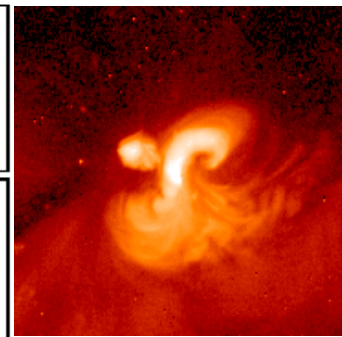
strong magnetic shear (Low 1977, Mikic & Linker 1994)



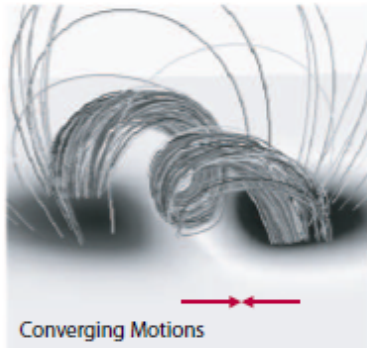
reversed shear (Kusano et al. 2004)



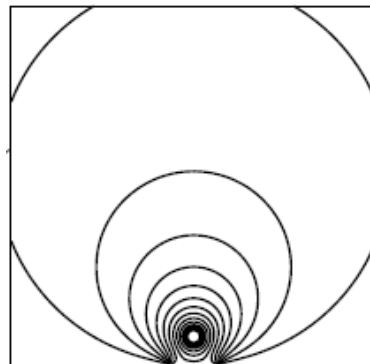
sigmoid & kinking (Rust & Kumar 1996, Canfield et al. 1999, Moore et al. 2001, Kliem et al. 2004)



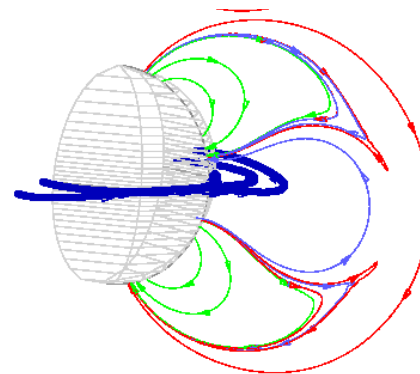
emerging fluxes (Heyvaerts et al. 1977; Wallace et al. 2010)



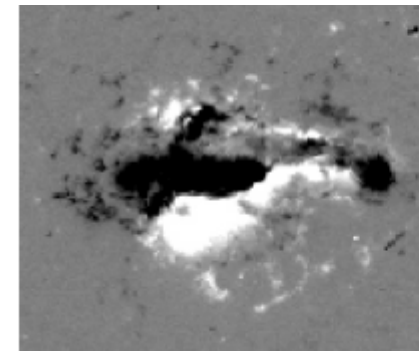
flux cancellation (van Ballegoijen & Martens 1989, Amari 1999, 2000, Green et al. 2011)



Loss-of-equilibrium model (Priest & Forbes 2002)

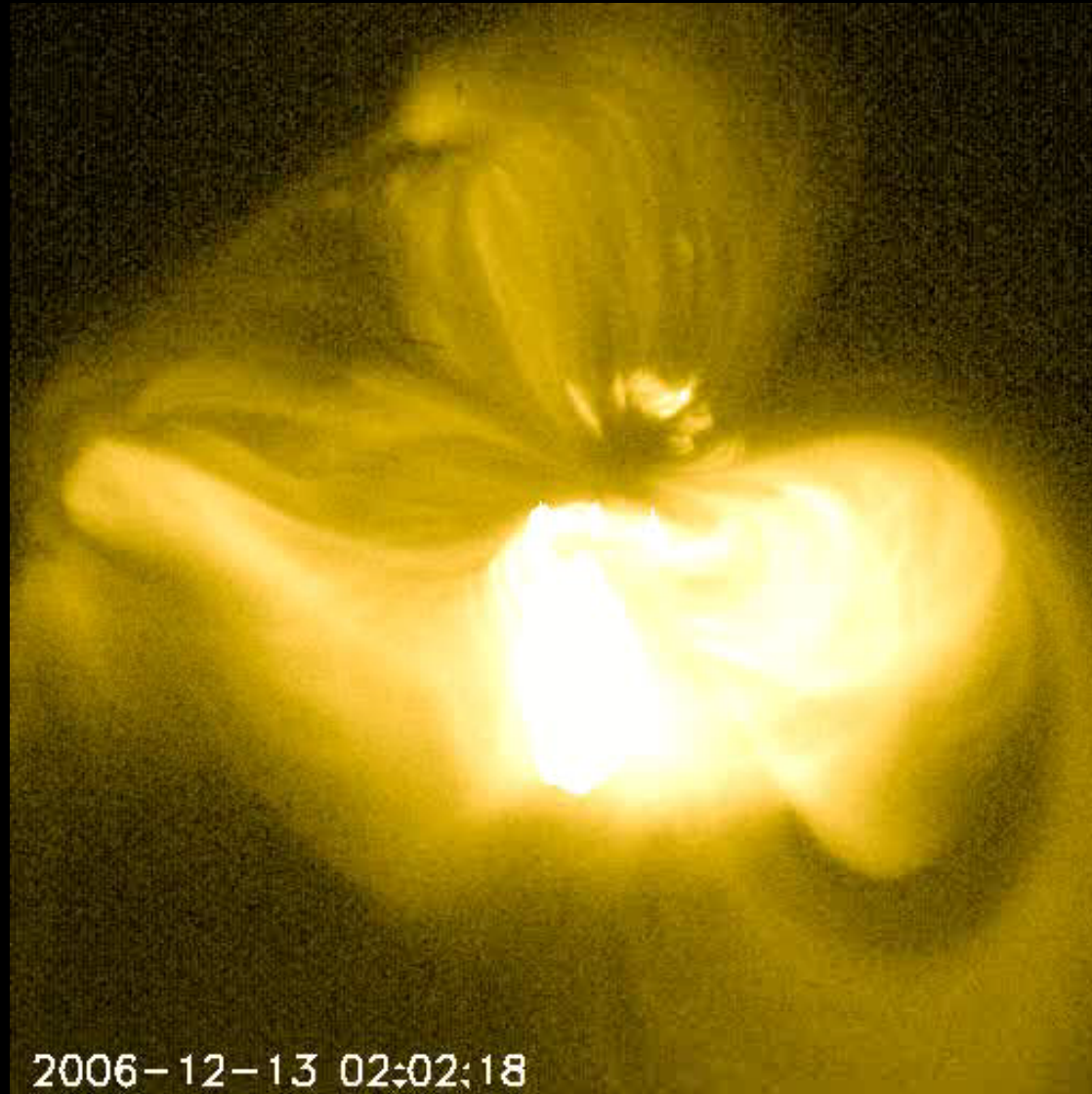


Breakout in multipolar topologies (Antiochos et al. 1999, Sterling & Moore 2004)



sharp gradient of B (Schrijver 2007)

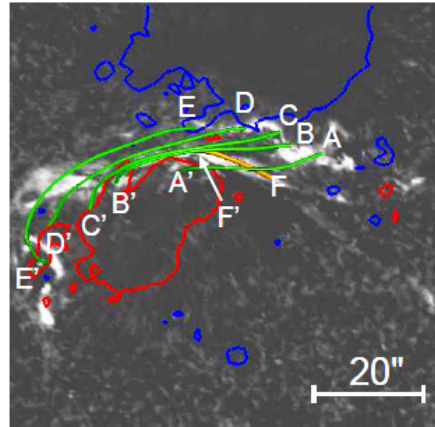
Hinode Flare



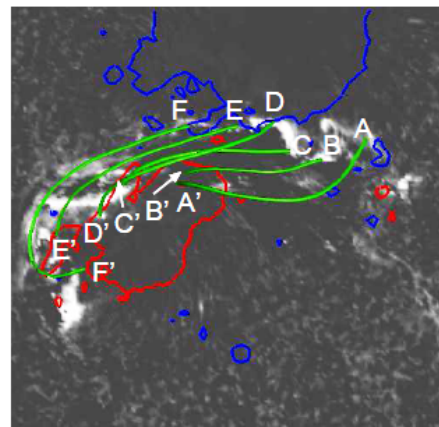
Stability of Active Region

Inoue, Kusano et al. ApJ 2011

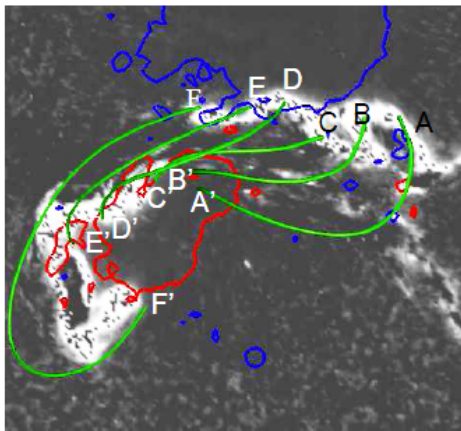
(a) 02:18 UT on Dec.13



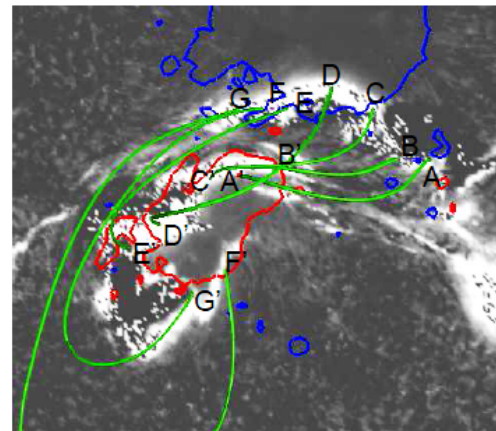
(b) 02:20 UT on Dec.13



(c) 02:22 UT on Dec.13



(d) 02:24 UT on Dec.13



Magnetic field at 20:30UT on Dec.12, 2006
Flare onset at 02:12UT on Dec.13, 2006

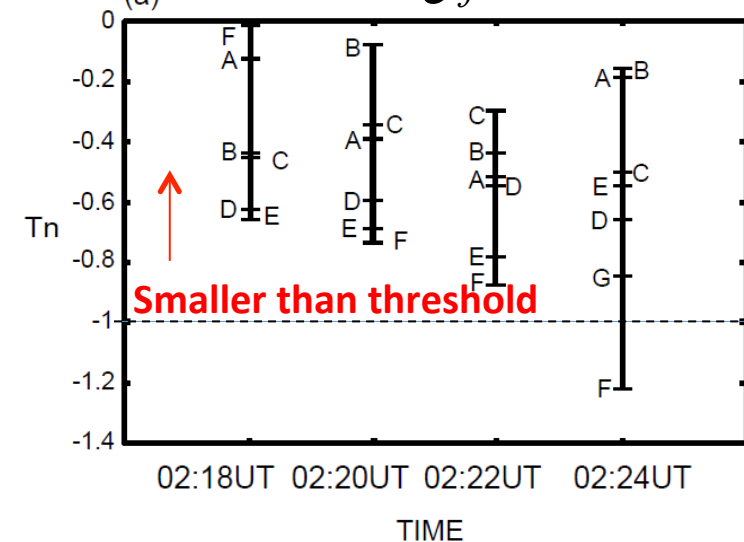
Hinode/SOT

Vector Magnetogram

NLFFF

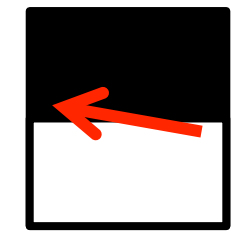
Magnetic Twist

$$T_n = (4\pi)^{-1} \int_{field\ line} \alpha dl$$

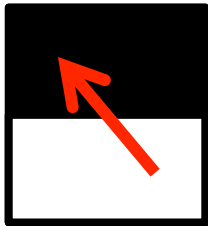


Ensemble Simulation Study

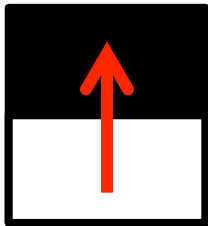
Kusano+2012



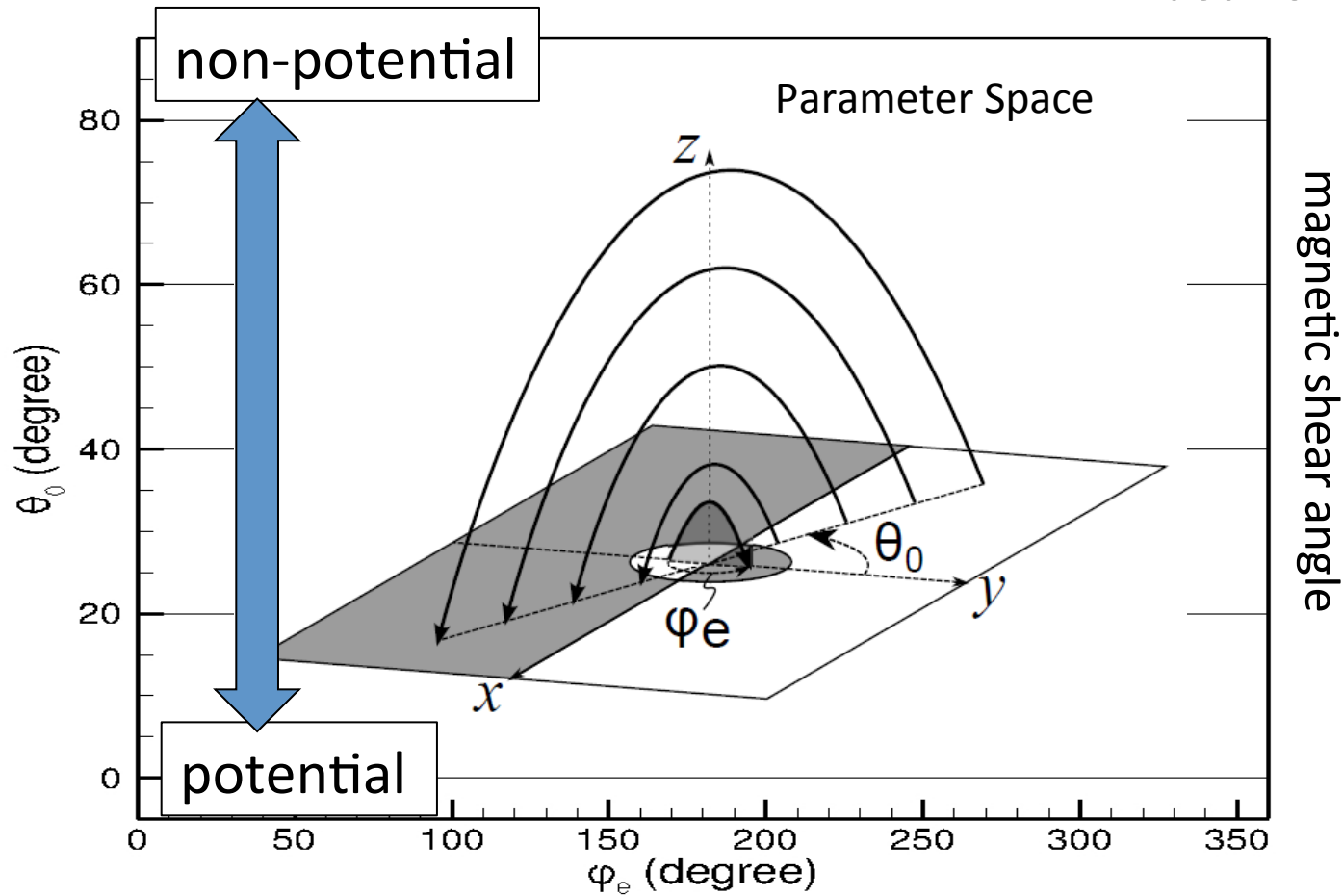
strong shear



weak shear

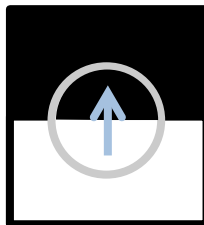


potential field

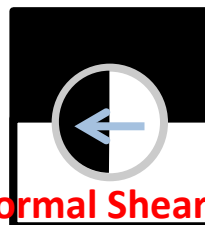


azimuth angle of small magnetic disturbance

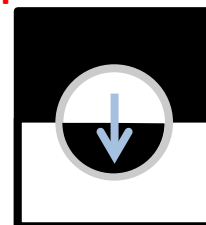
Right Polarity



Opposite Polarity

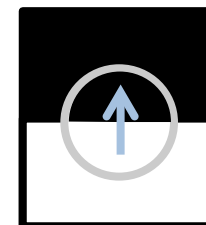


Normal Shear



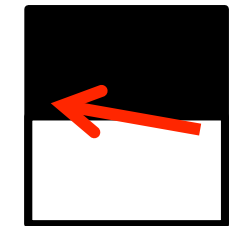
Reversed Shear

Right Polarity

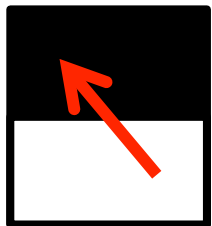


Simulation Results

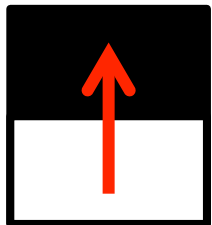
Flare phase diagram (Kusano et al. 2012)



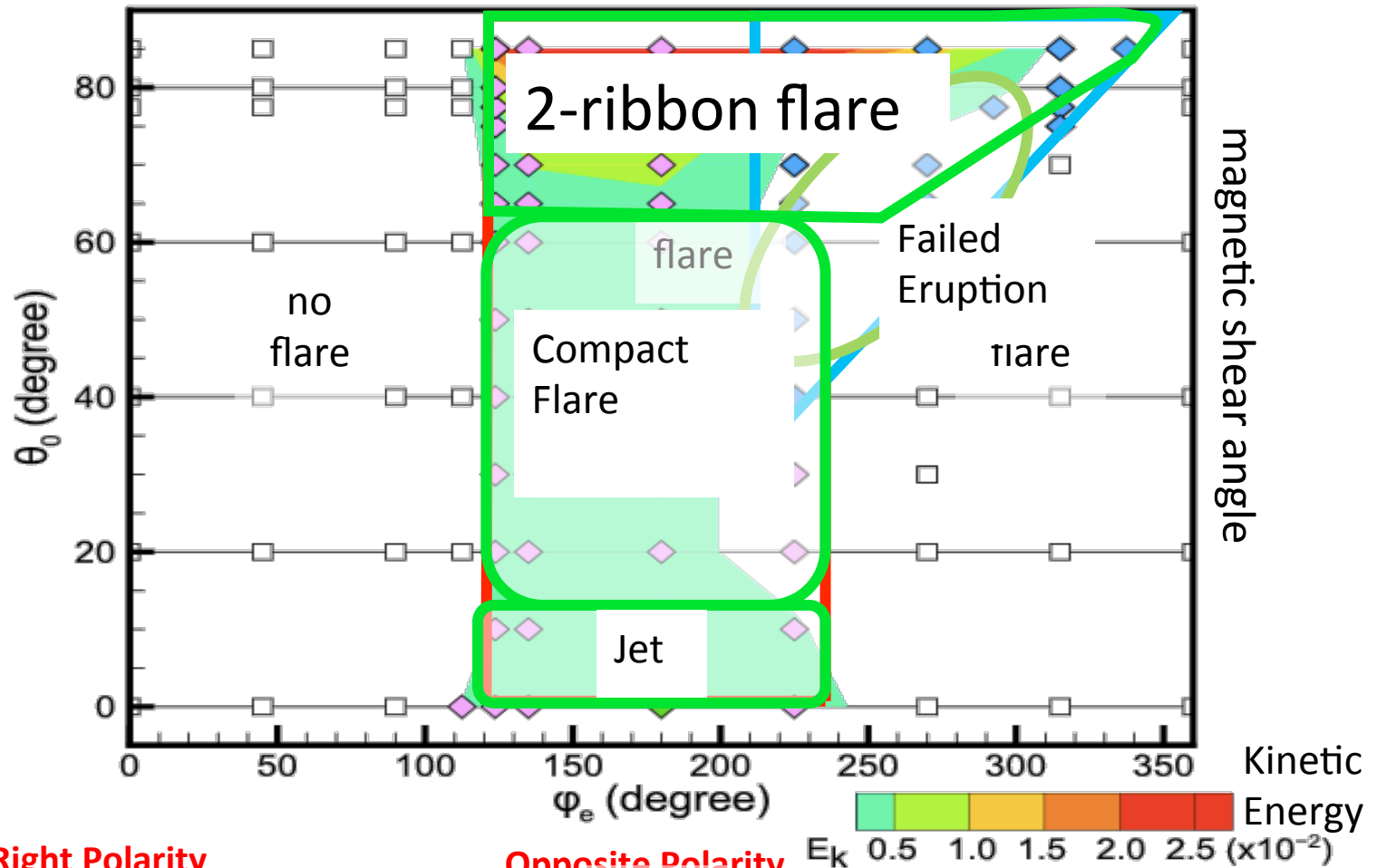
strong shear



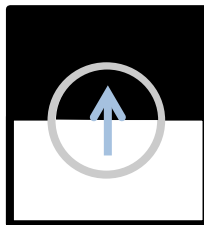
weak shear



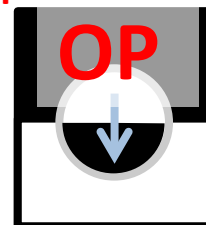
potential field



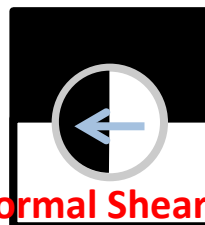
Right Polarity



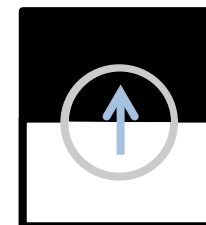
Opposite Polarity



Normal Shear

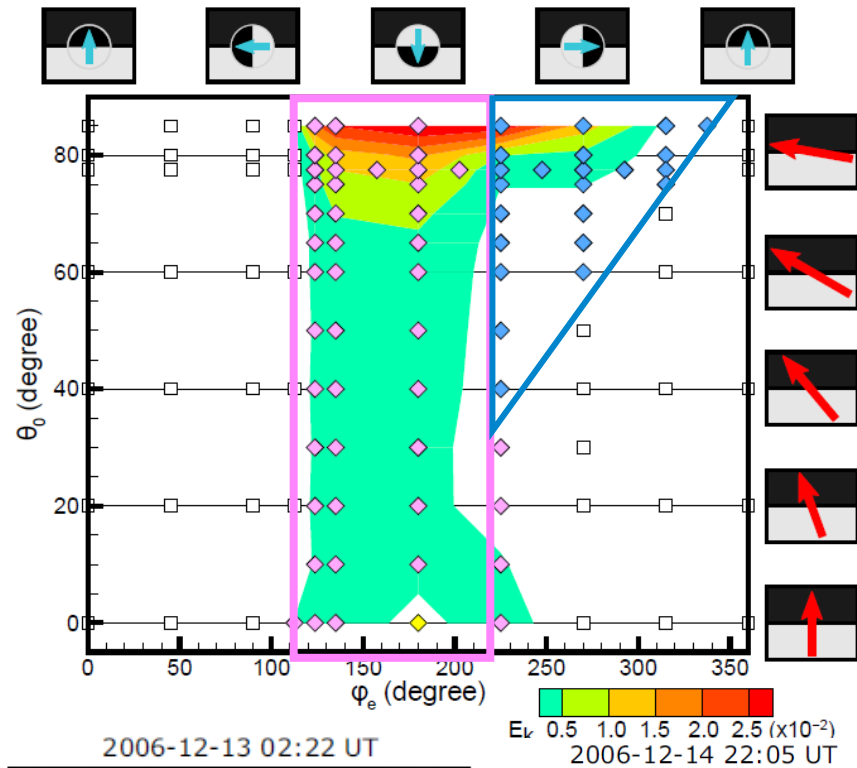


Reversed Shear

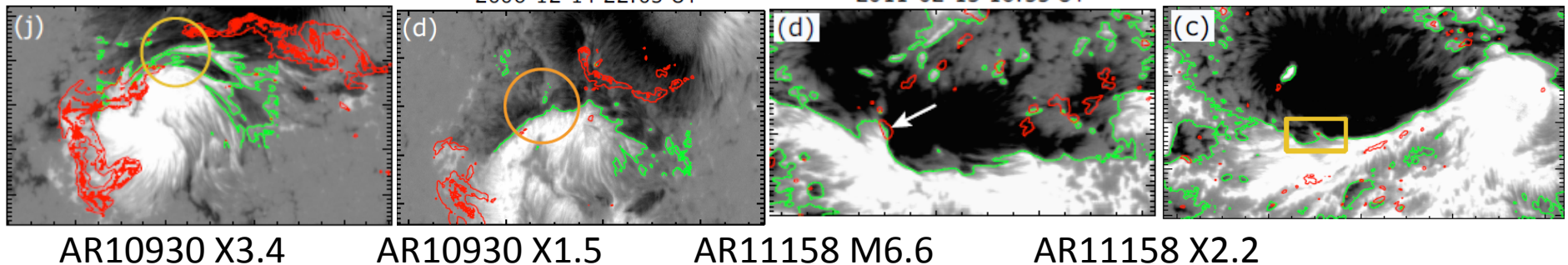
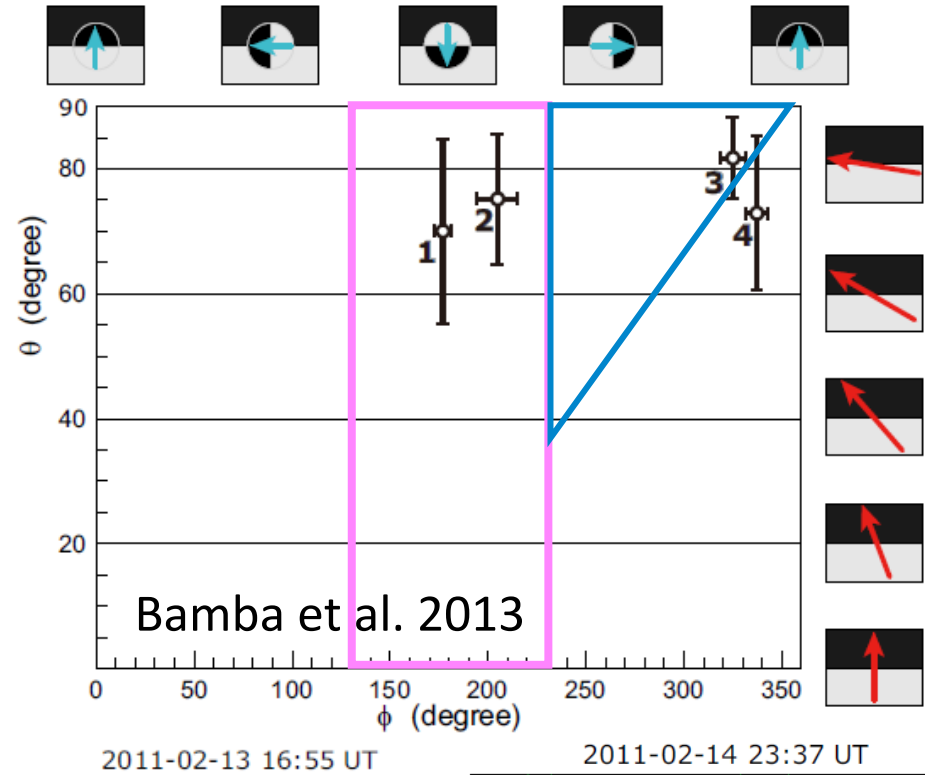


Observational Evidence

Simulation (flare phase diagram)

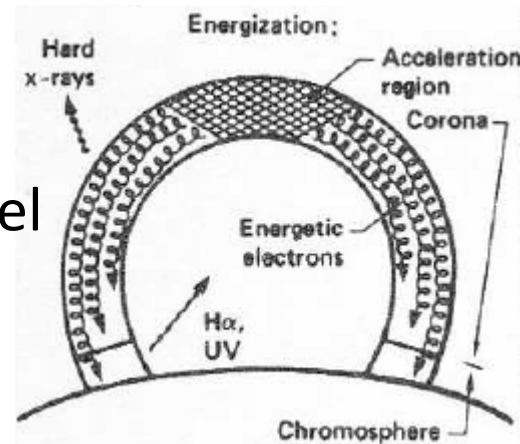


Observation (Hinode)

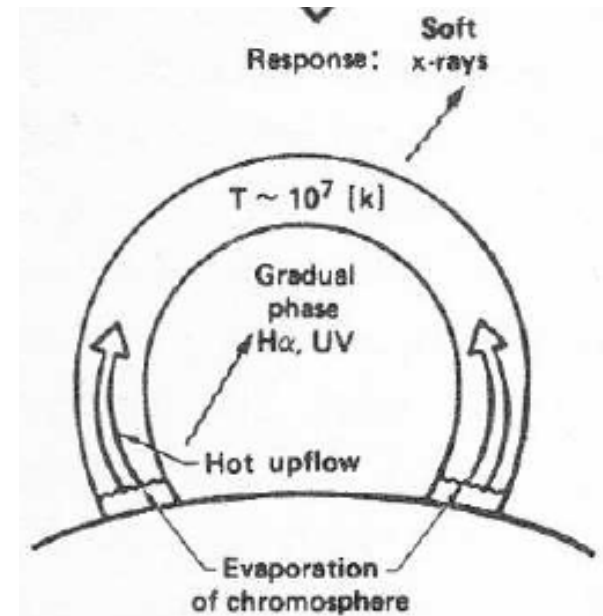
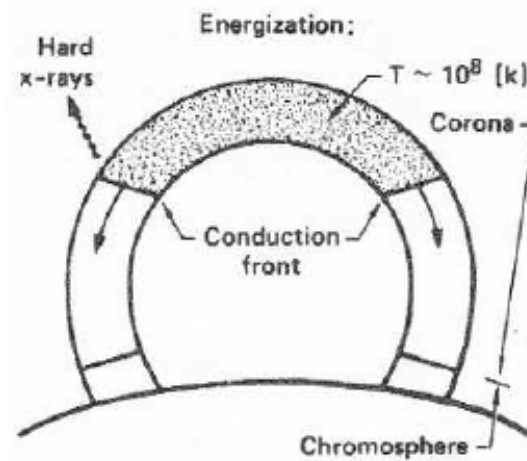


Chromospheric evaporation

Non-thermal
thick-target model

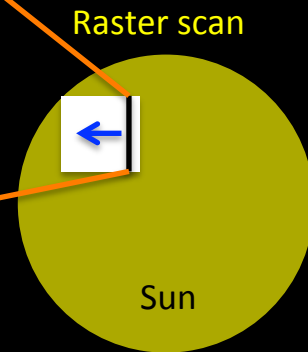
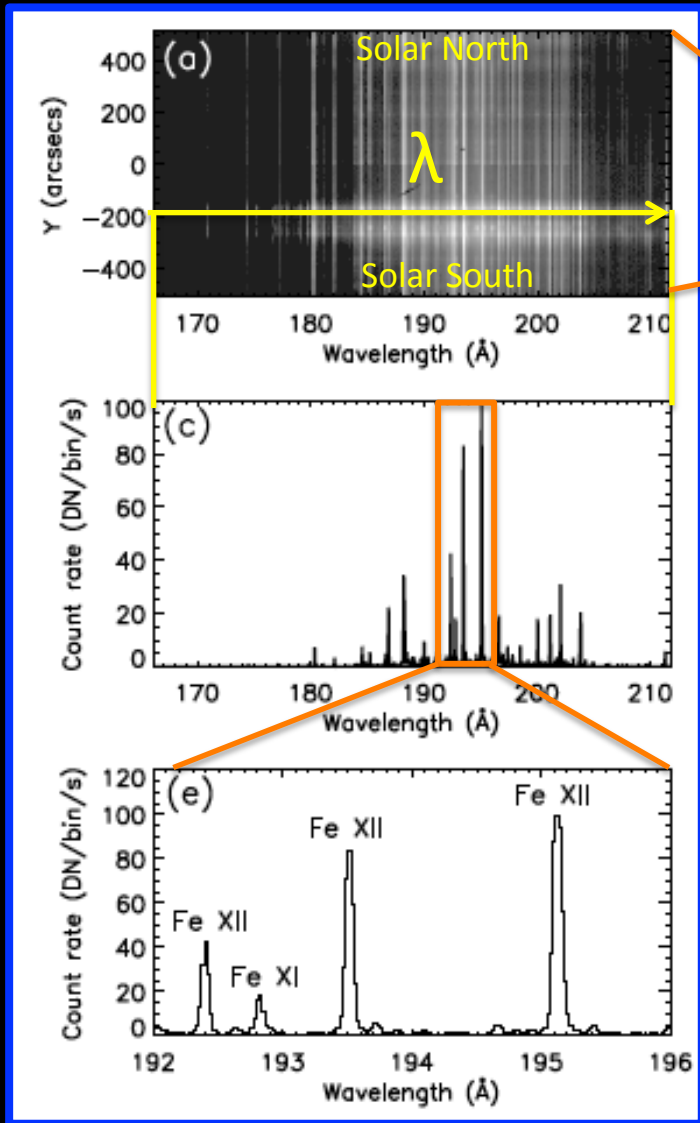


Thermal model

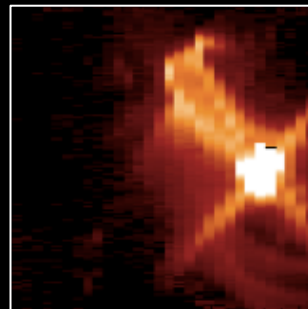


From Fisher (1986)

EUV imaging spectrograph



time
 t_{32} t_{20} t_{10} t_1



Example of Raster scan image



2006 -

Slit of both spectrographs is oriented in the north-south direction.

Chromospheric Evaporation studied by plenty of EUV spectral lines

Mostly studied from EIS data.

- T_e dependent flow speed
Milligan & Dennis (2009)
Watanabe et al. (2010)
Chen & Ding (2010)
Li & Ding (2010)

- High density at the footpoints
from density sensitive line ratio

Fe XIII-XIV: $10^{10.5} \text{ cm}^{-3}$ (Watanabe et al. 2010)

Fe XII-XIV: $10^{11.5} \text{ cm}^{-3}$ (Milligan 2011)

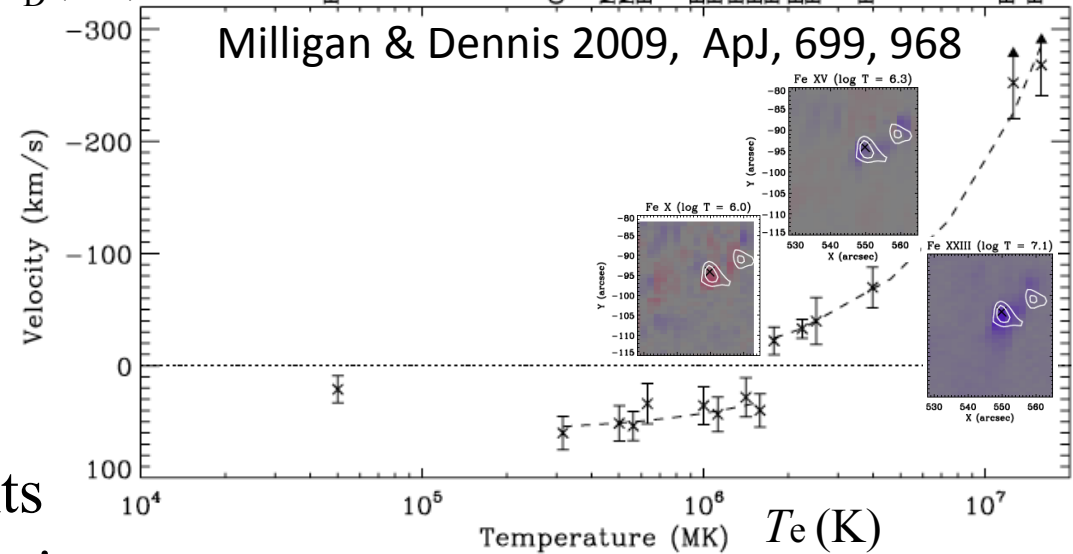
Fe XIV : 10^{11} cm^{-3} (Del Zanna et al. 2011)

High-density kernels are in a narrow layer $\leq 200 \text{ km}$

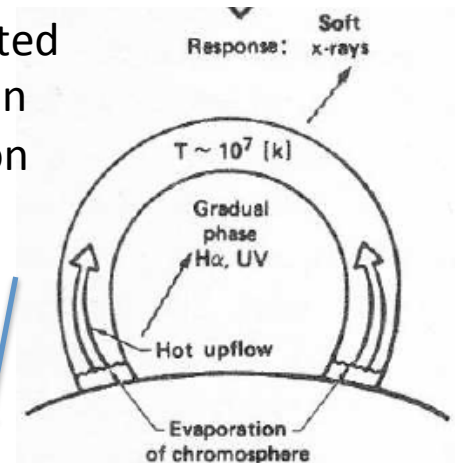
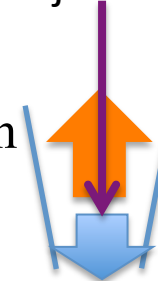
Fe XIII : $10^{10.3} \text{ cm}^{-3}$ (Graham et al. 2011)

Doppler velocity

V_D (km/s)

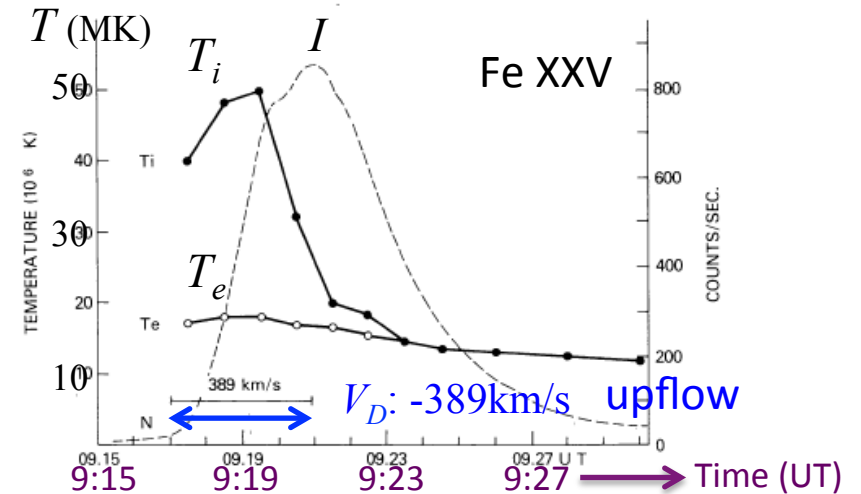
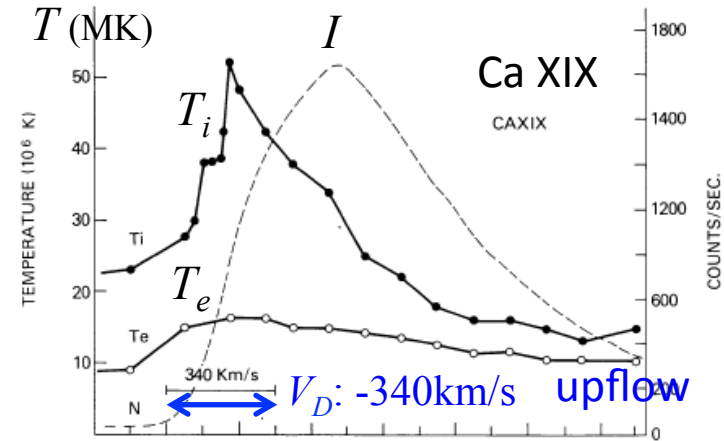
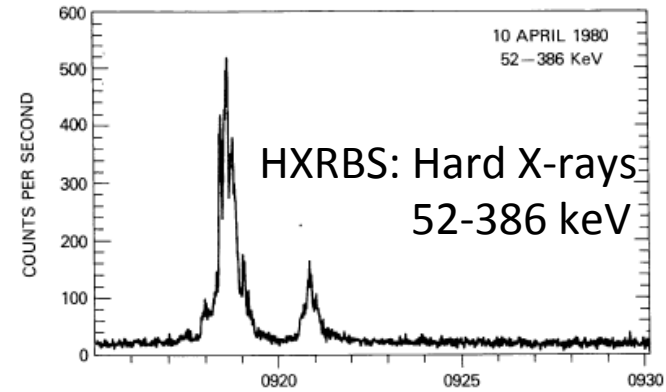
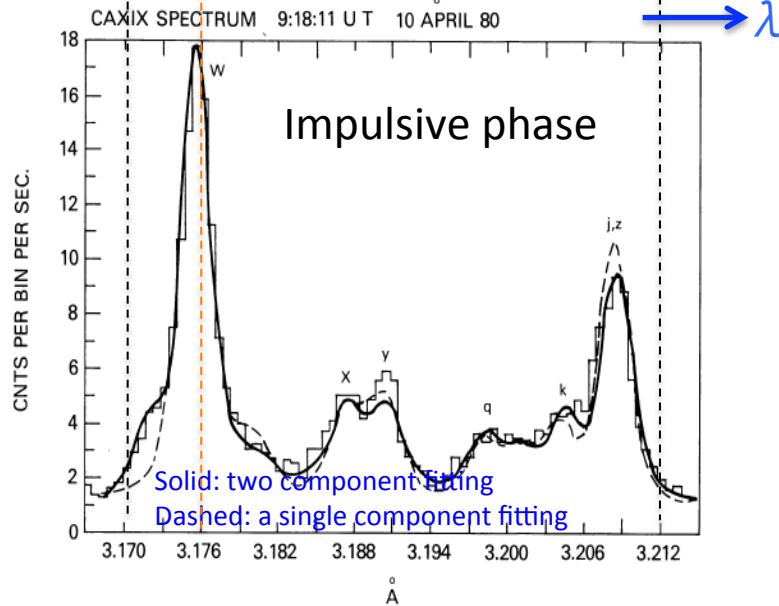
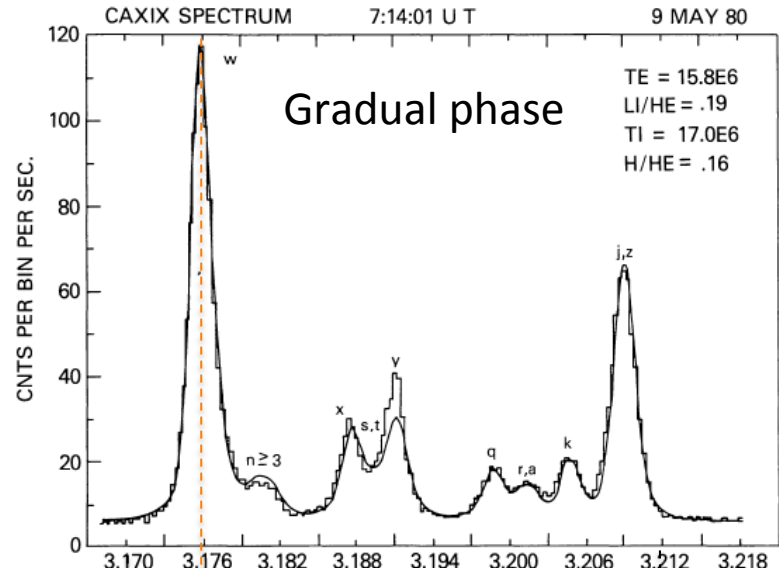


Accelerated
electron
injection



Non-thermal broadening

SMM/BCS: Antonucci et al. (1982)

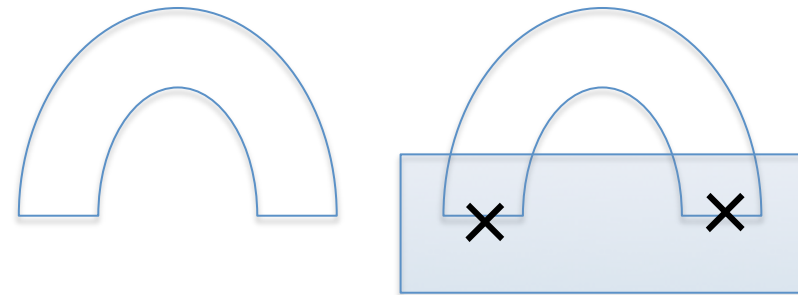
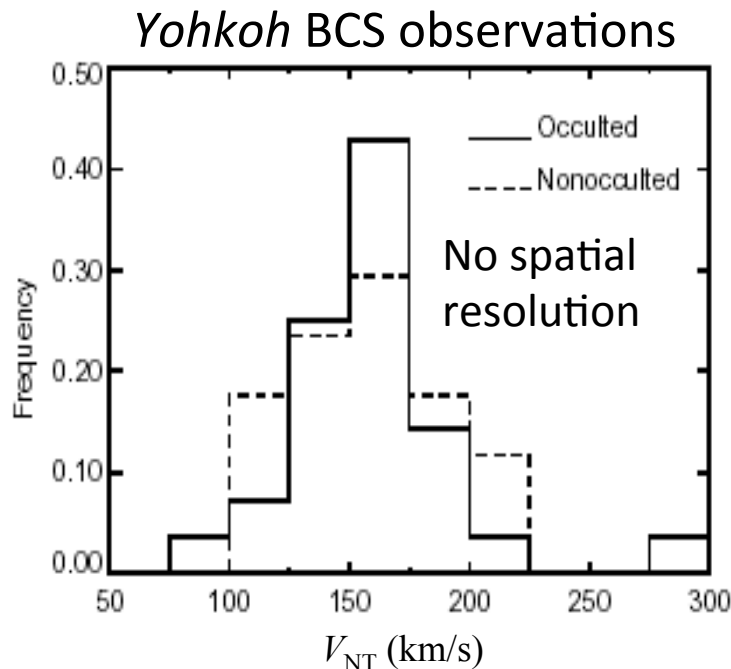


Non-thermal Velocity in Flares

- Site of non-thermal velocity observed in flaring loops and its size has not been understood.

$$W_{\text{obs}} = \sqrt{W_1^2 + 4 \ln 2 \left(\frac{2kT_i}{M_i} + V_{\text{NT}}^2 \right)} \equiv \sqrt{W_1^2 + W^2}$$

W_{obs} : observed FWHM of an emission line



Occulted flare by the disk at the limb

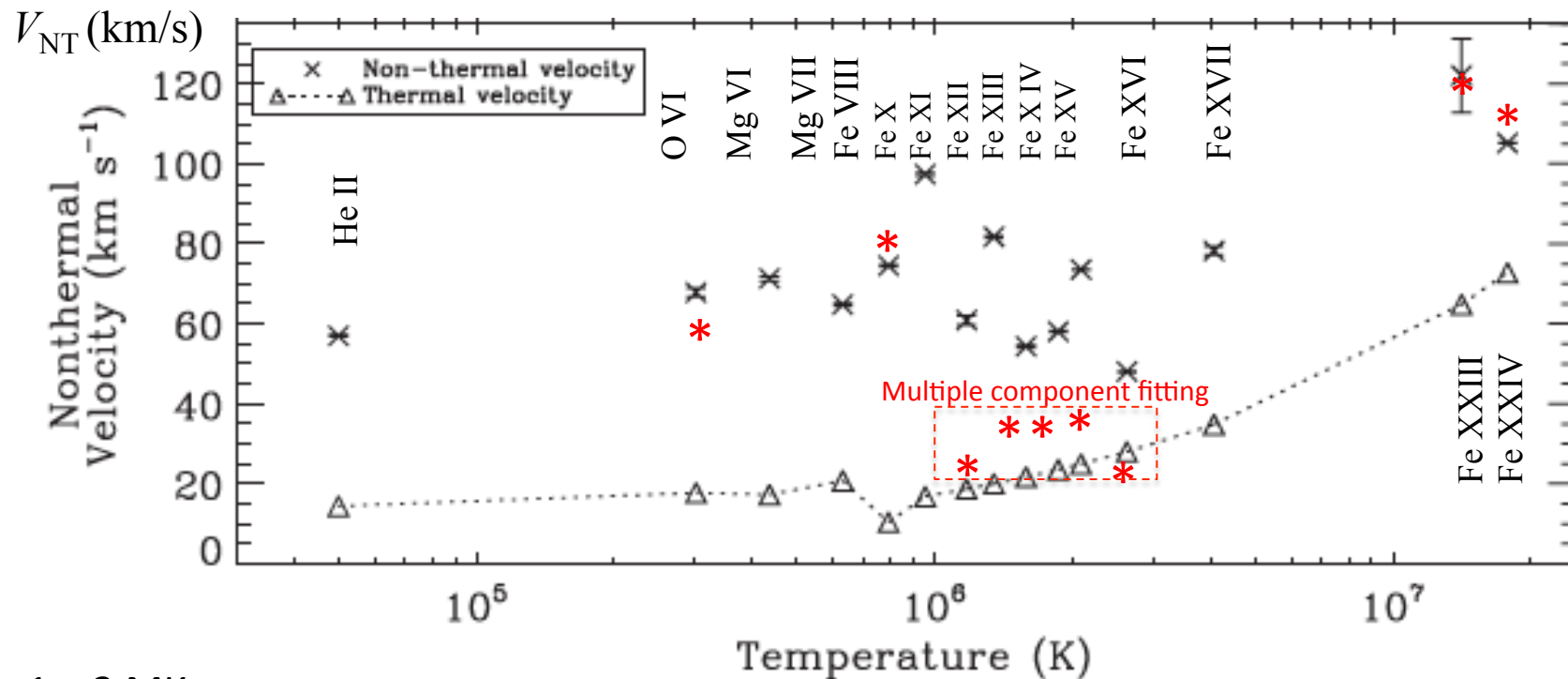
From Mariska and McTiernan 1999, ApJ, 514, 484-492

FIG. 5.—Normalized histograms of the peak nonthermal broadening velocity measured in the BCS Ca XIX channel for each flare listed in Tables 1 and 2.

V_{NT} at the footpoints

from Non-thermal broadening of emission lines at Flare Kernel

Milligan (2011), Young et al. (2013)



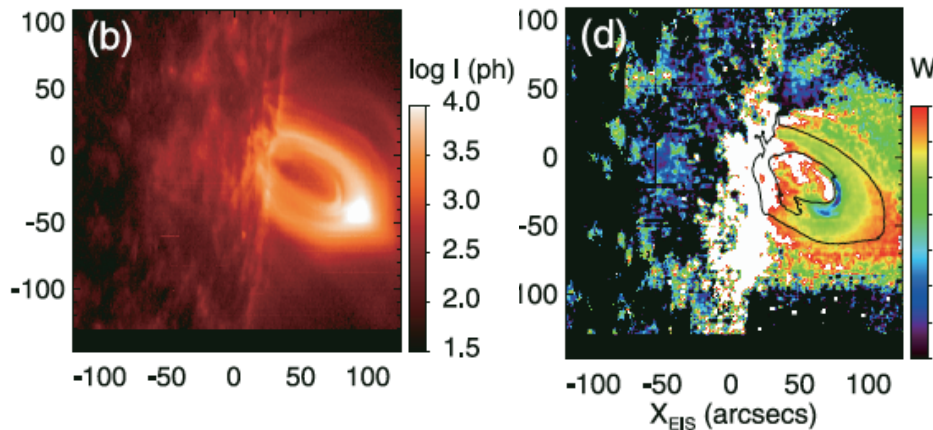
1 – 3 MK range:

Milligan (2011): unresolved flow structures, turbulence (?)

Young+ (2013): multiple flow component (upflow and downflow simultaneously detected)

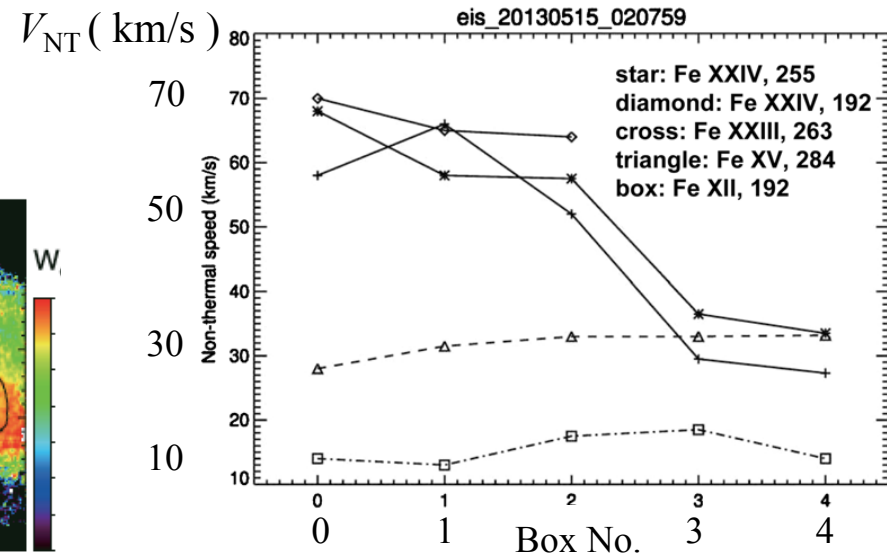
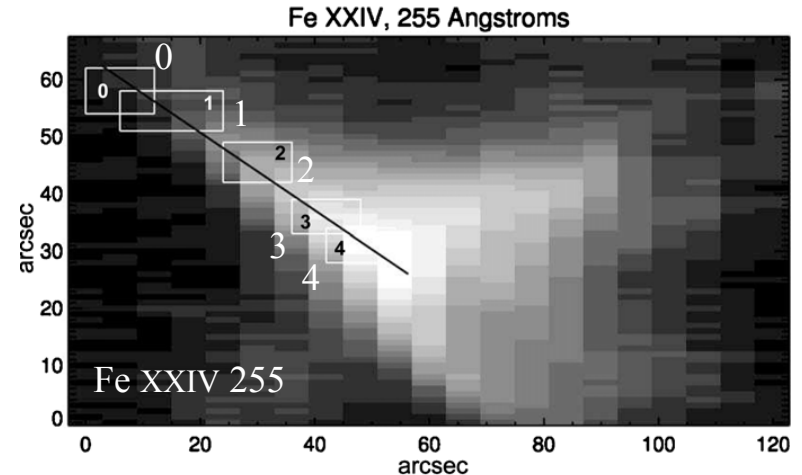
V_{NT} at/above the loop tops

- Impulsive phase:
 - $V_{NT} = 100 - 230$ km/s
Hara et al. (2011, 2014)
Kawate & Imada (2013)
- Peak to late phase:
 - $V_{NT} = 40 - 70$ km/s
Hara et al. (2008)
Doschek et al. (2014)



Hara et al. (2008)

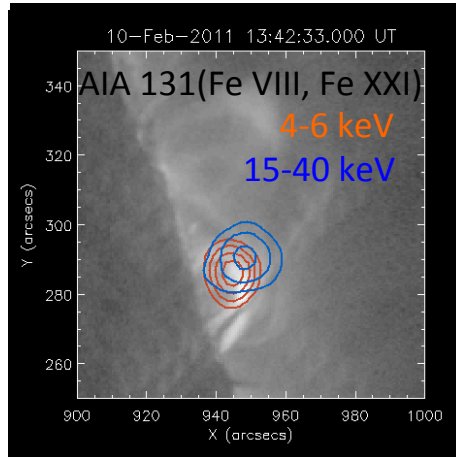
Late Phase of an X-class Flare



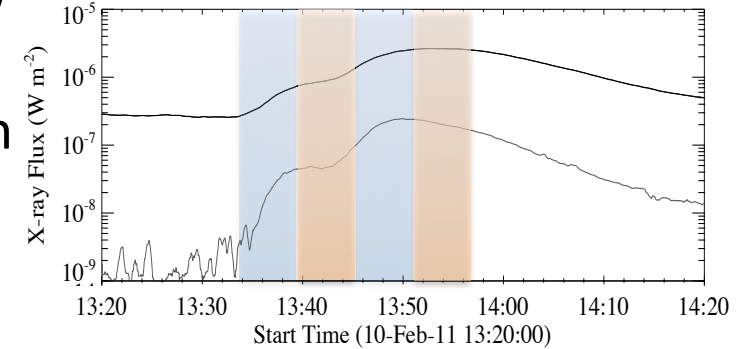
Doschek et al. (2014)

Line broadening at the loop top

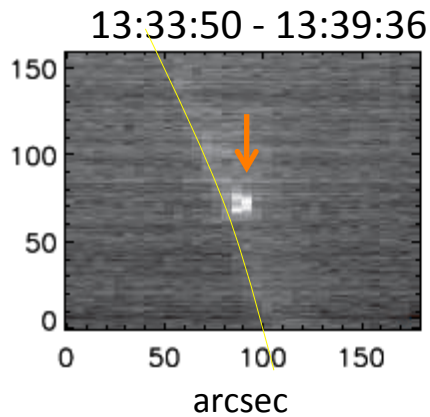
- a side view -



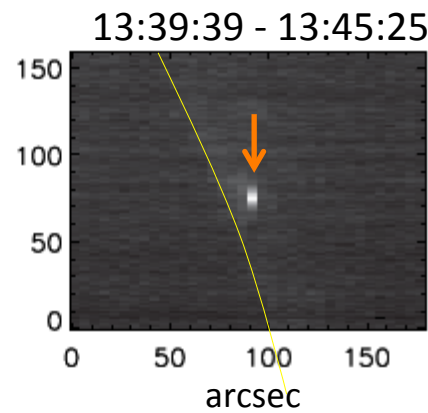
- Symmetric line profile with enhanced line broadening



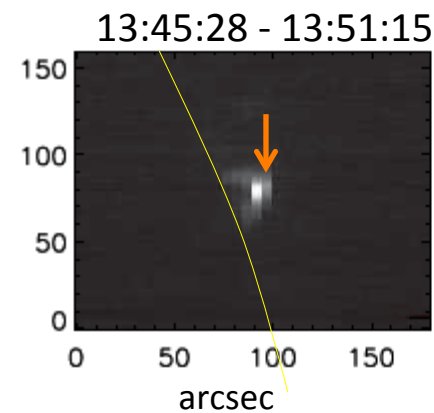
EIS: Fe XXIII 263.76 line intensity



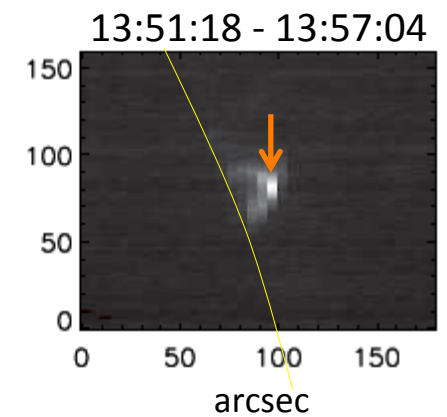
$T_e \sim 11\text{MK}$
 $T_i \sim 50\text{MK}$
 (or $V_{NT} \sim 110\text{ km/s}$)



$T_e \sim 11\text{MK}$
 $T_i \sim 20\text{MK}$
 (or $V_{NT} \sim 40\text{ km/s}$)



$T_e \sim 14\text{MK}$
 $T_i \sim 45\text{MK}$
 (or $V_{NT} \sim 100\text{ km/s}$)



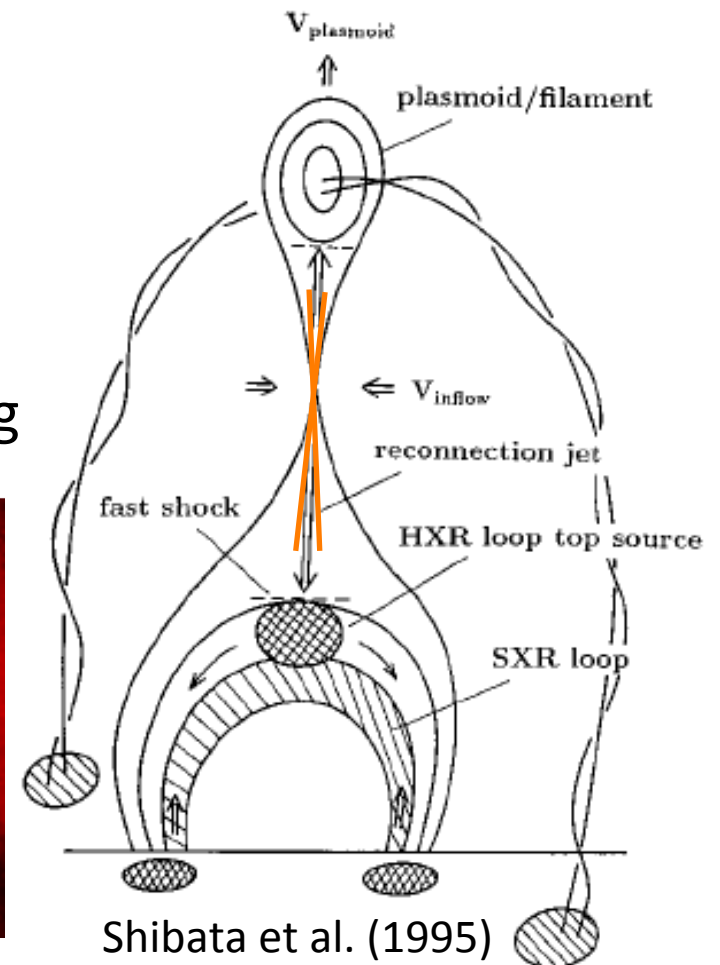
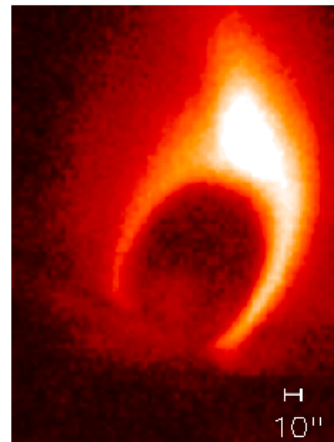
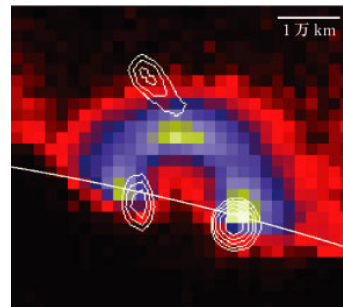
$T_e \sim 12\text{MK}$
 $T_i \sim 20\text{MK}$
 (or $V_{NT} \sim 40\text{ km/s}$)

Hara+ (2014)

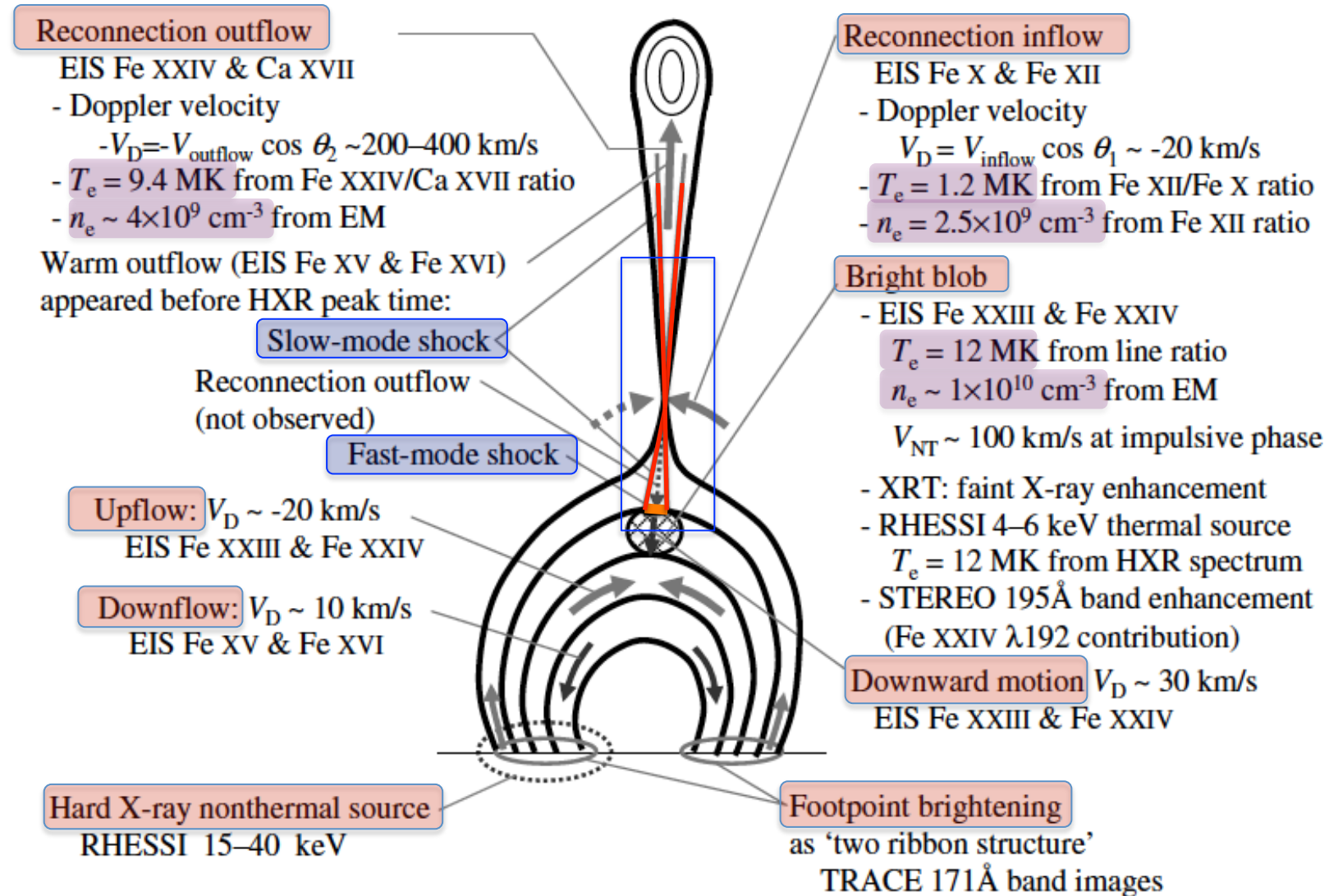
Magnetic Reconnection: a model based on *Yohkoh* imaging observations

Topics investigated by spectroscopy to understand magnetic reconnection processes in the solar atmosphere.

- Reconnection inflow
- Reconnection outflow/plasmoid
- Position of enhanced hot line broadening found in 1970s
- MHD Shock



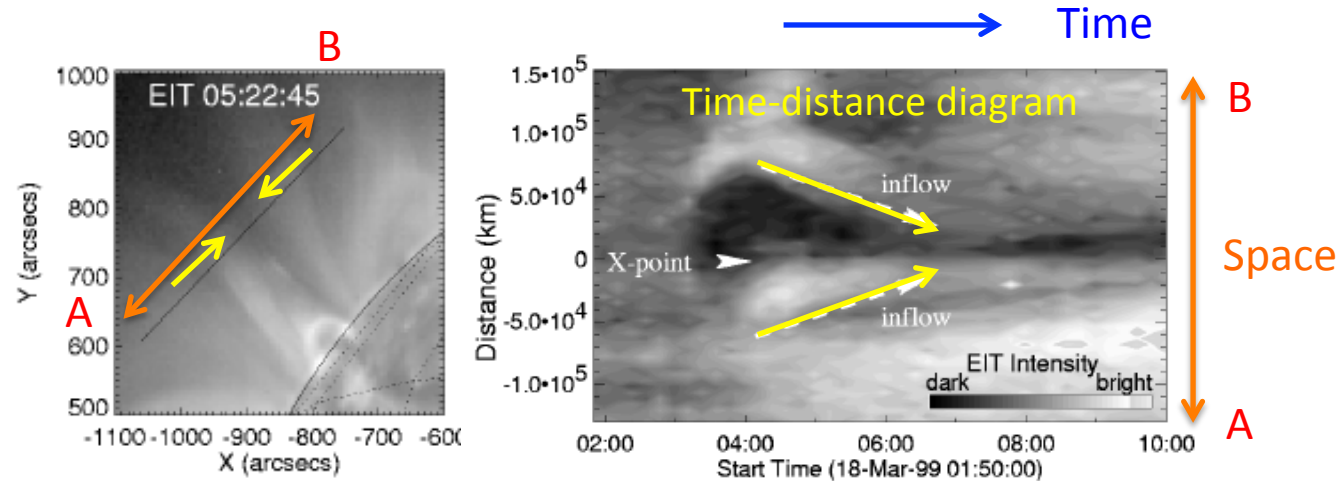
Observed & Suggested Structures in 2007 May 19 Flare (GOES B9.5)



$$V_{\text{inflow}} / V_{\text{outflow}} = (V_{D, \text{inflow}} / V_{D, \text{outflow}}) (\cos \theta_2 / \cos \theta_1) = 0.067 (\cos \theta_2 / \cos \theta_1)$$

Reconnection Inflow

EUV Imaging Observations: Reconnection Inflow

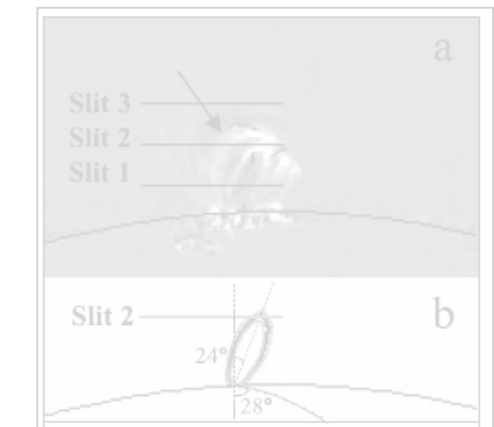
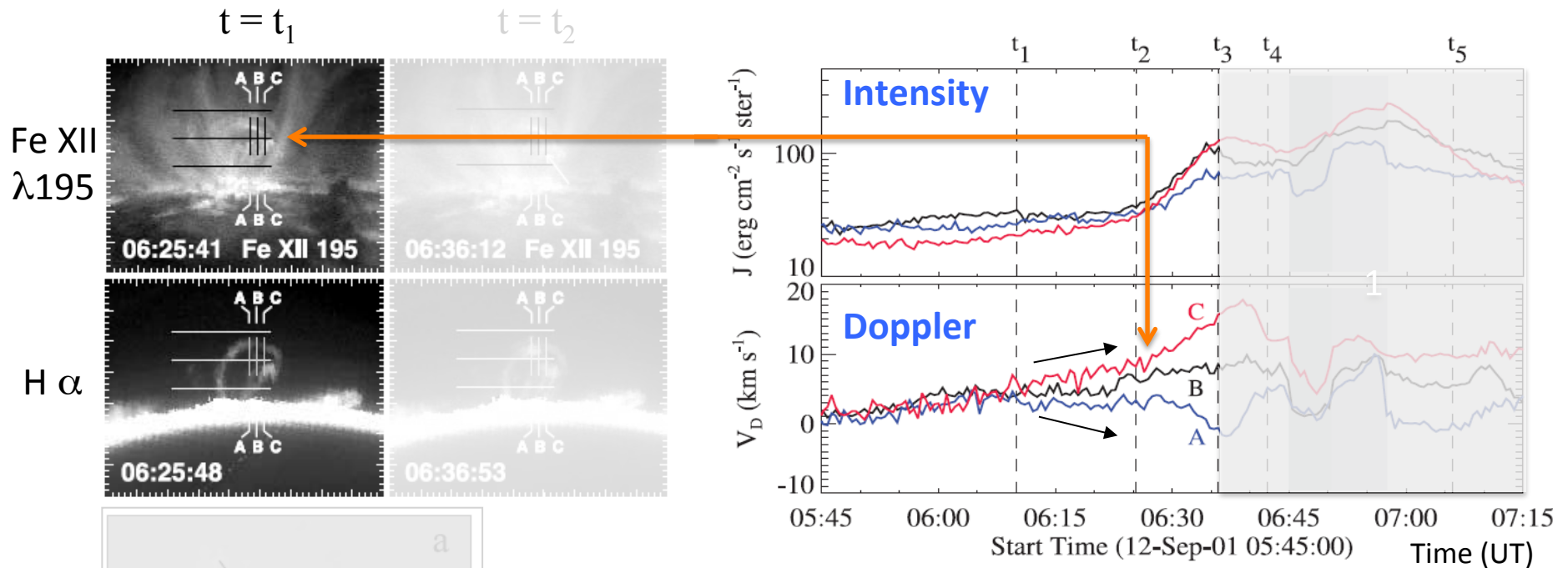


SOHO/EIT Observation

Yokoyama et al. (2001)

- Yokoyama et al. (2001)
 - Estimation of inflow speed from apparent motion of coronal structures around a flare
 - $V_{\text{inflow}} \sim 5 \text{ km/s}$, $M_A = V_{\text{inflow}}/V_A = 0.001-0.03$ (uncertainty in V_A)
- Narukage & Shibata (2006); 6 events
 - $V_{\text{inflow}} = 2-14 \text{ km/s}$, $M_A = V_{\text{inflow}}/V_A = 0.001-0.07$

First Spectroscopic Observation of Reconnection Inflow

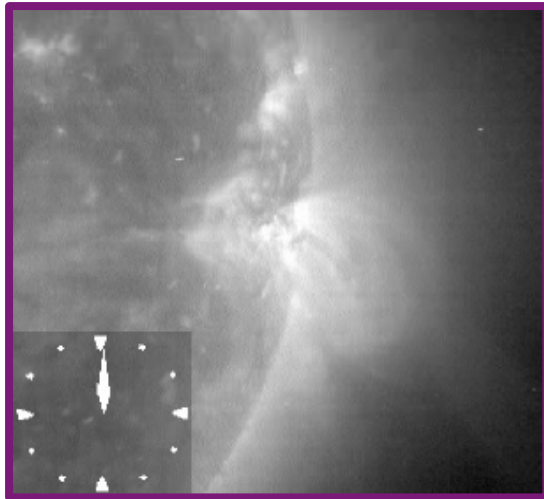


Difference of EUV images

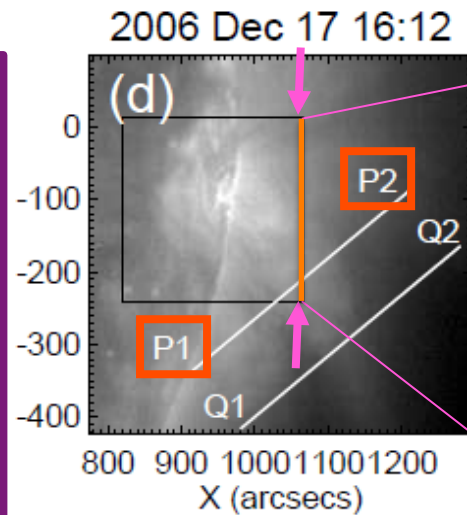
- Fe X 6374 observation at Norikura Solar Observatory of NAOJ ($\lambda/\Delta\lambda=1E5$) [Hara et al. 2006, ApJ, 648, 728]
- $V_{D, \text{inflow}} \sim 3 \text{ km/s}$ [observation]
- $M_A \sim 0.003$ when $V_A \sim 1000 \text{ km/s}$ in the corona [assumption in B]

EIS Spectroscopic Observations:

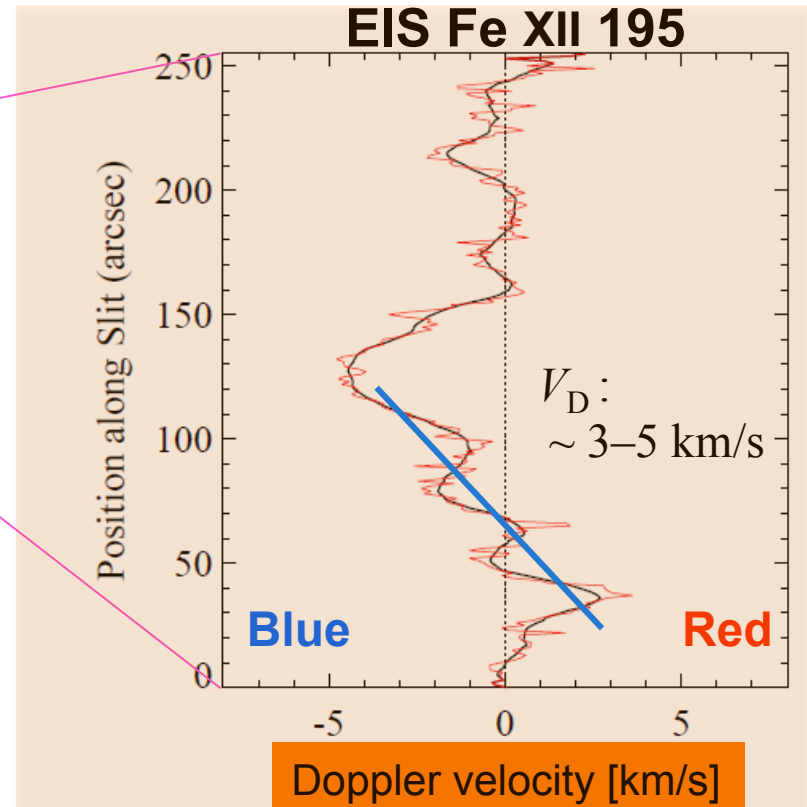
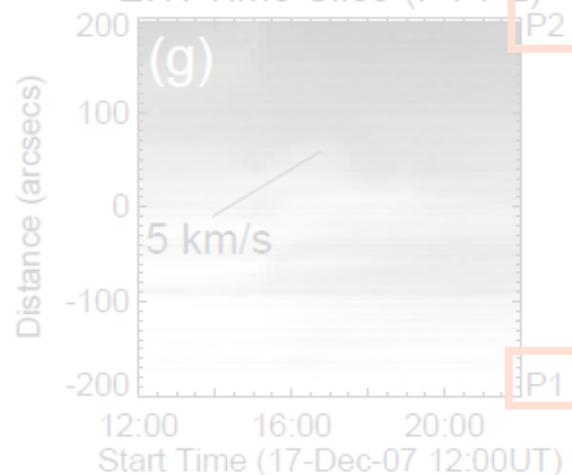
- Reconnection Inflow in an eruptive event -



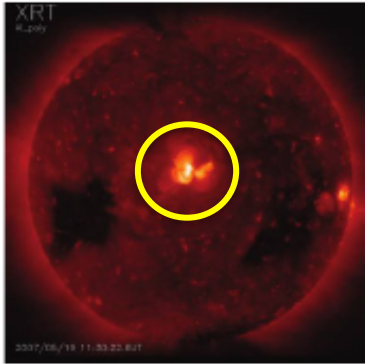
GOES C2.1



EIT: Time Slice (P1-P2)

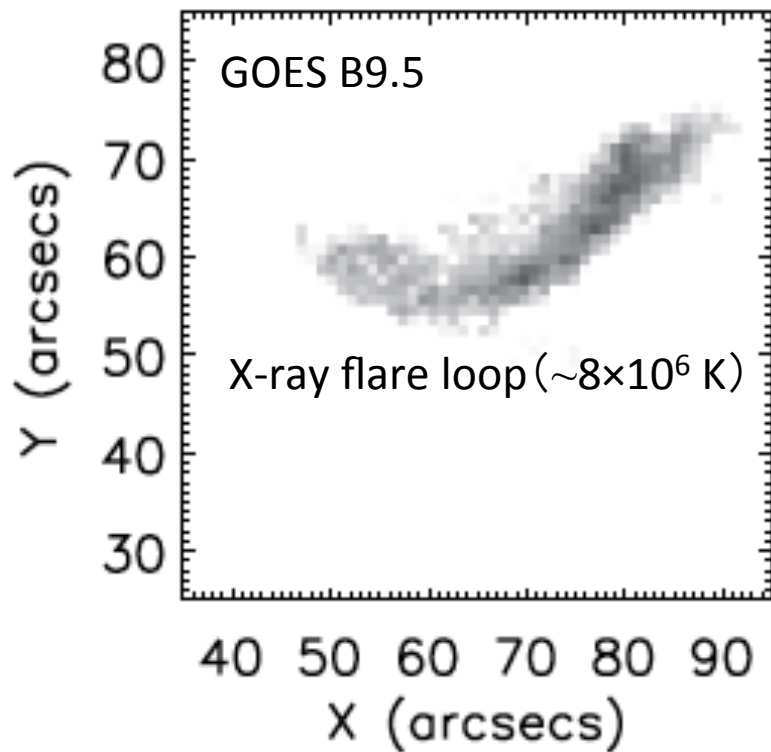


- Weak Doppler signature of inflow
- No multiple observations to prove
- No 10^7 K line observations



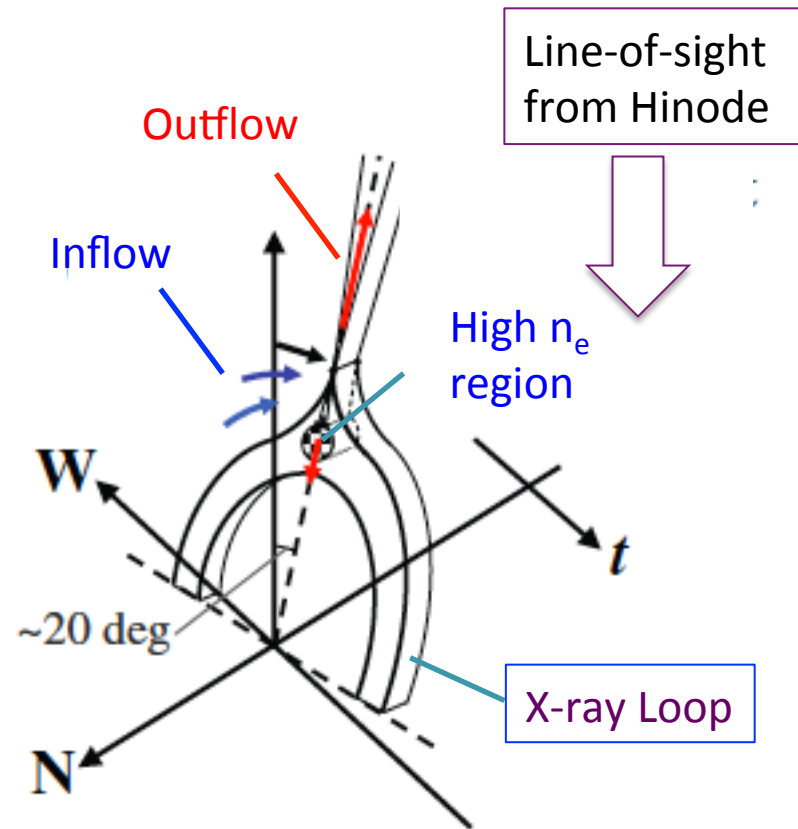
Magnetic Reconnection in an eruptive event

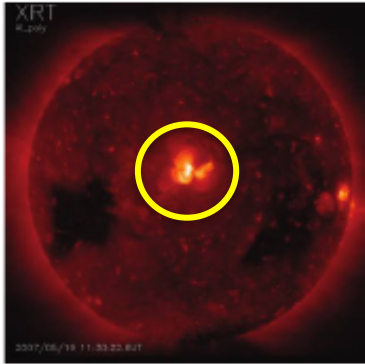
N



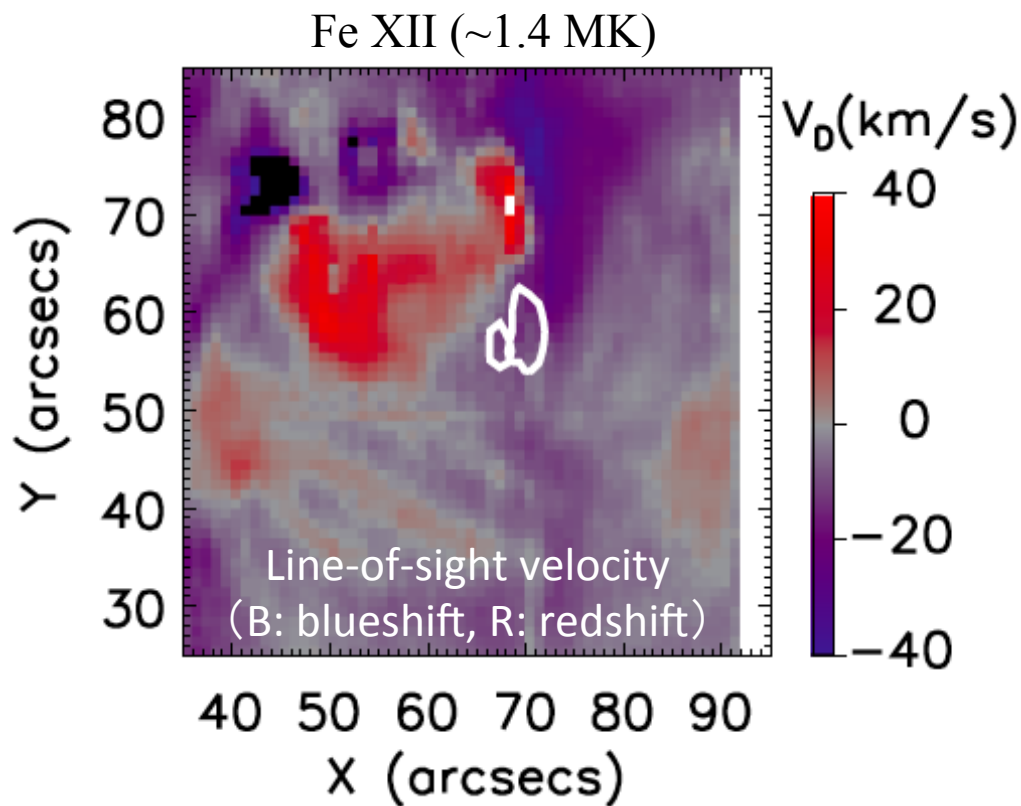
W

1 arcsec = ~ 700 km on the Sun

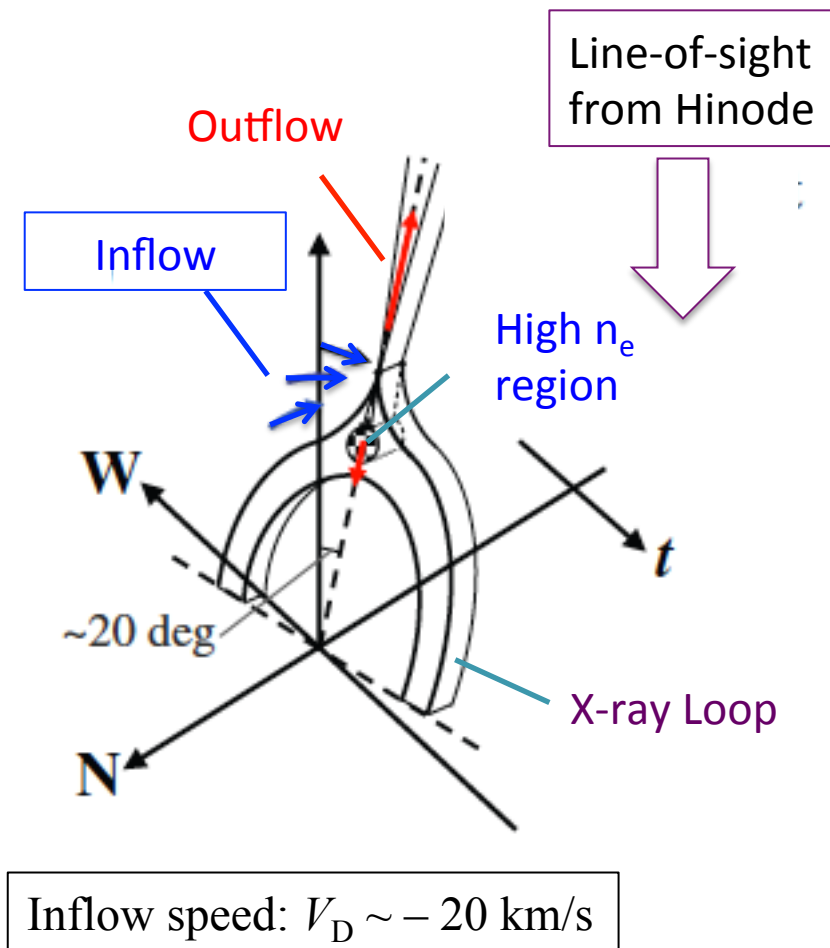




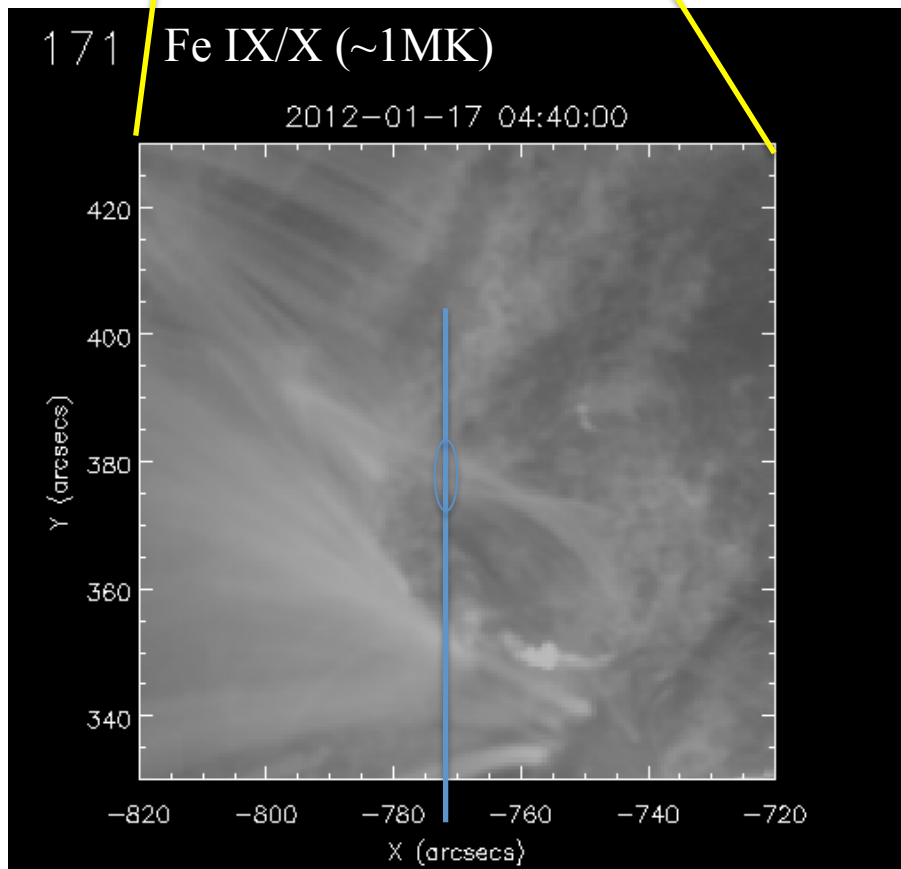
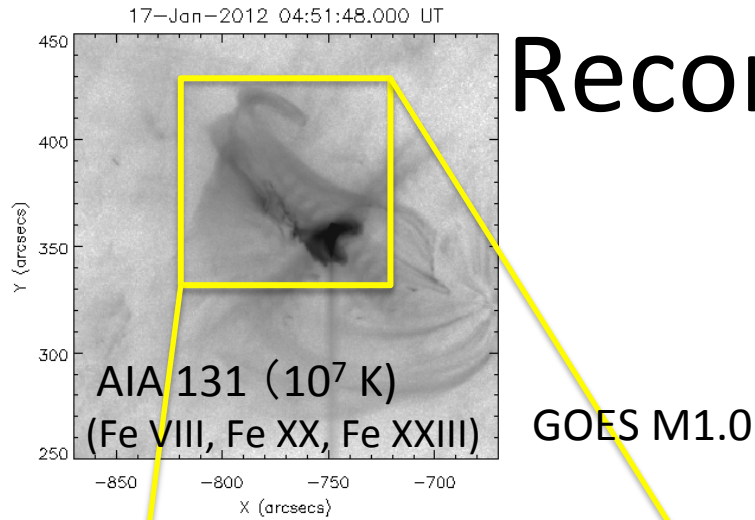
Magnetic Reconnection in an eruptive event



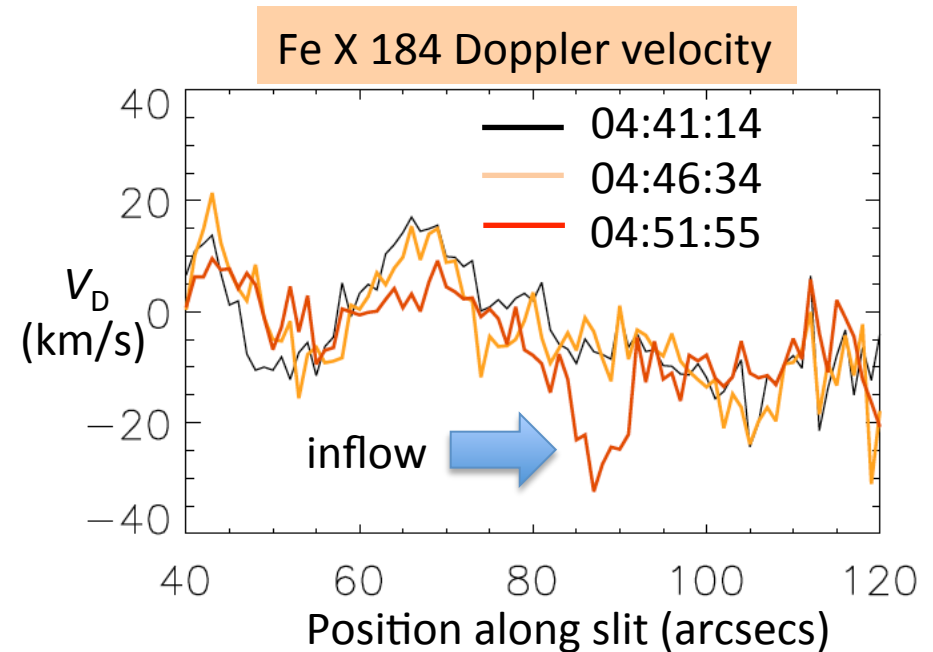
1 arcsec = ~ 700 km on the Sun



Reconnection Inflow

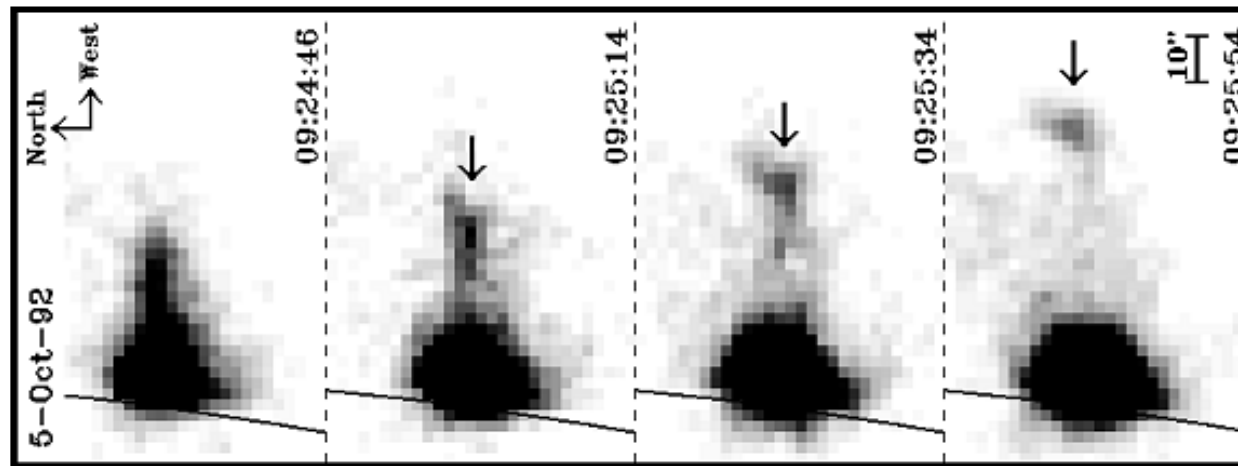
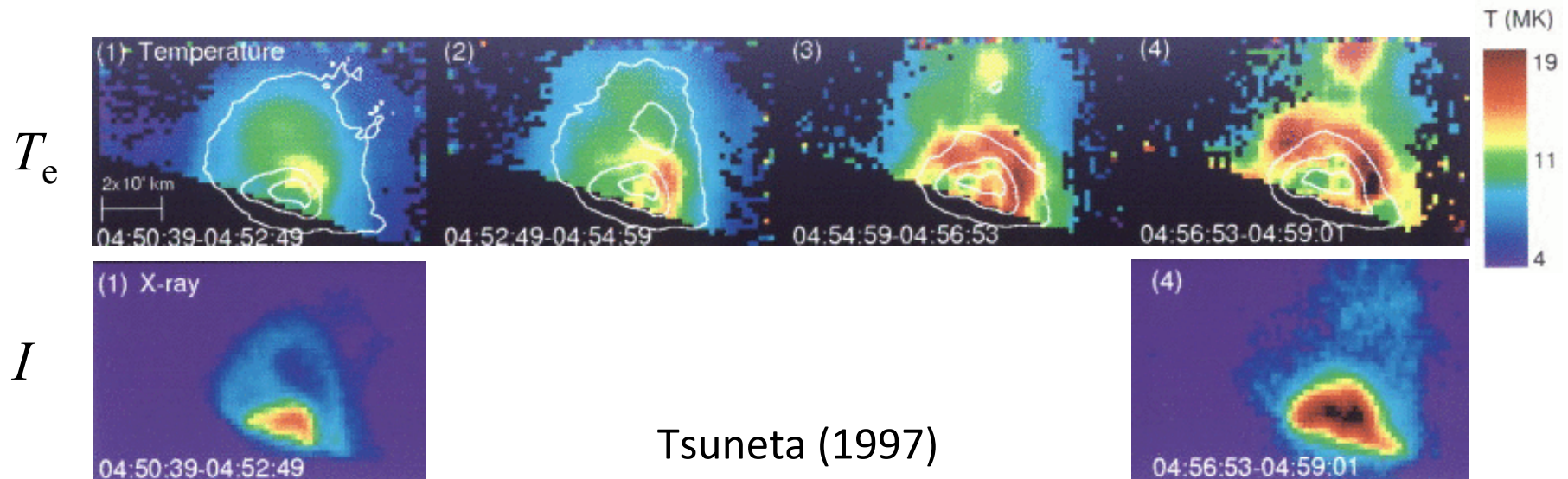


- Signature of reconnection inflow structure was observed in AIA171 as a disappearing loop: apparent speed ~ 50 km/s
- EIS observed blueshift of -25 km/s and intensity decrease in Fe X 184.
- $M_A \sim V_{\text{inflow}}/V_{\text{outflow}} \sim 0.1$



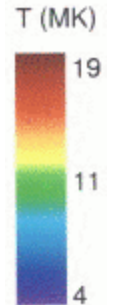
Reconnection Outflow/Plasmoids

Yohkoh Imaging Observations: Plasma Ejections



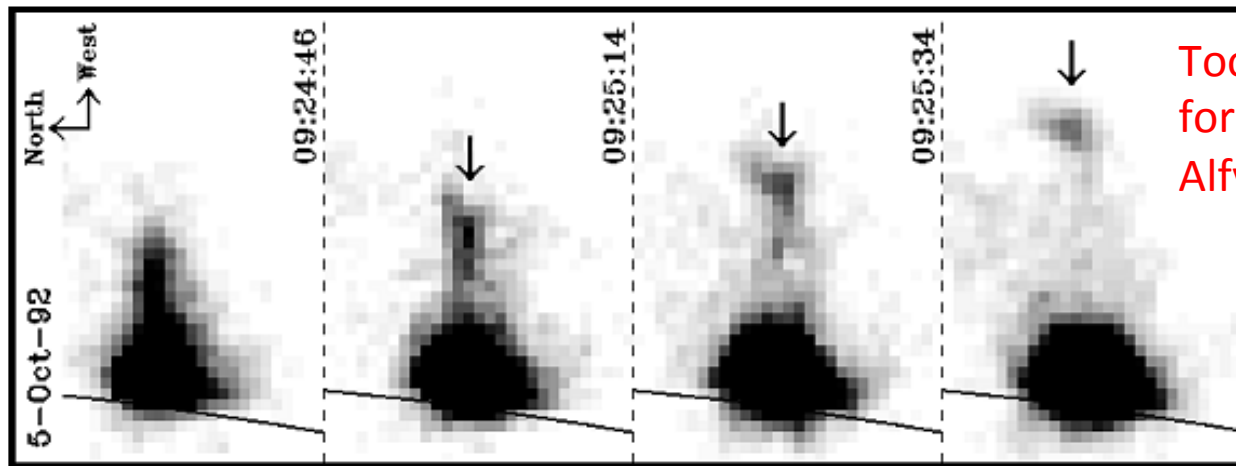
SUMMARY OF EIGHT COMPACT-LOOP LIMB FLARES

Date	Peak Time (UT)	GOES Class	Height of HXR Source above SXR Loop	Ejection	Apparent Velocity of Ejection (km s^{-1})
1991 Dec 2	0455	M4	$<5''$	Yes	50–150
1992 Jan 13	1729	M2	$5''-10''$	Yes	100–150
1992 Feb 6	0325	M8	At apex	Yes	30–70
1992 Feb 17	1542	M2	$<5''$	Yes	50–150
1992 Apr 1	1014	M2	No loop top	Yes	130–170
1992 Oct 4	2221	M2	$5''-10''$	Yes	300–370
1992 Nov 5	0620	M2	No loop top	Yes	100–150
1993 Feb 17	1036	M6	$5''-10''$	Yes	100–150



T_e

I



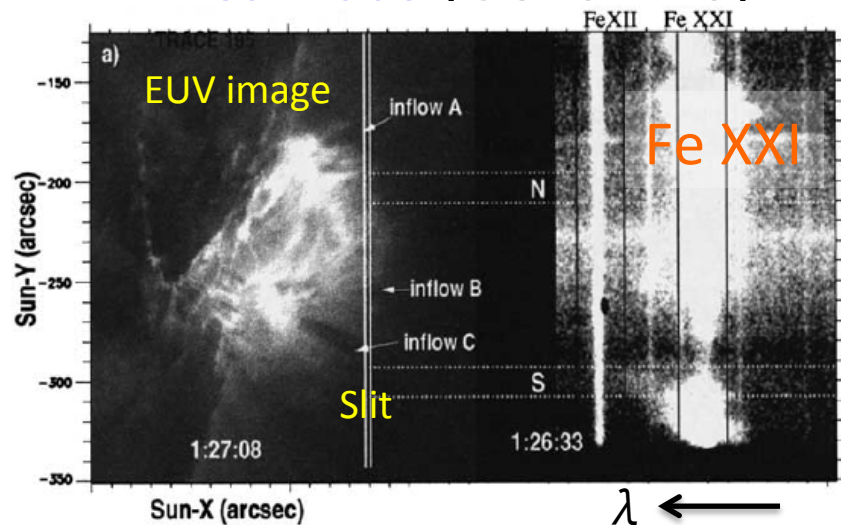
Too slow for coronal Alfvén speed

Ohyama & Shibata (1998)

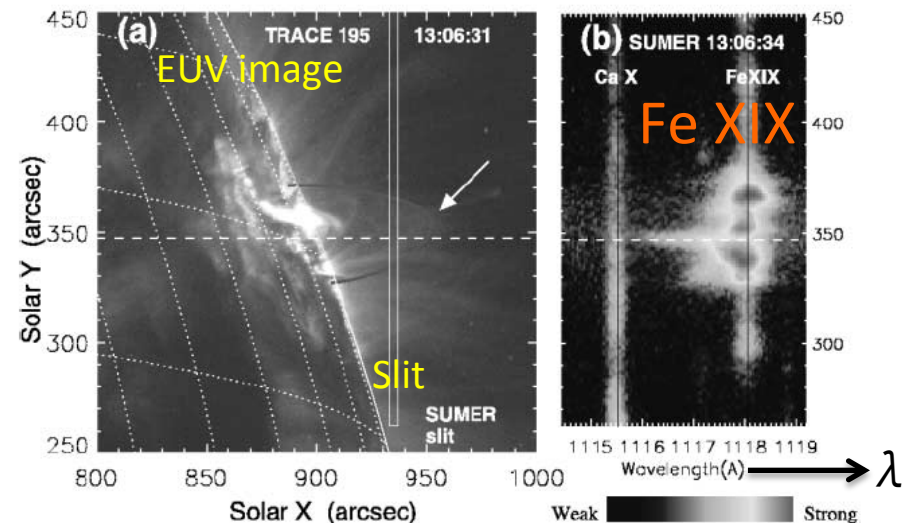
Reported EUV Observations of Reconnection Outflows

- A few cases have only been reported on the spectrum of reconnection outflow. **A dark structure in general.**
 - SOHO/SUMER: Innes+2003 (X1.5) Fe XXI } No scanning observations
 - Wang+2007 (M2.5) Fe XIX }
 - Hinode/EIS: Hara+2011 (B9.5) Fe XXIV, Fe XXIII, Ca XVII
 - Imada+2013 (X1.7) Fe XXIV

Innes+2003 (GOES X1.5)



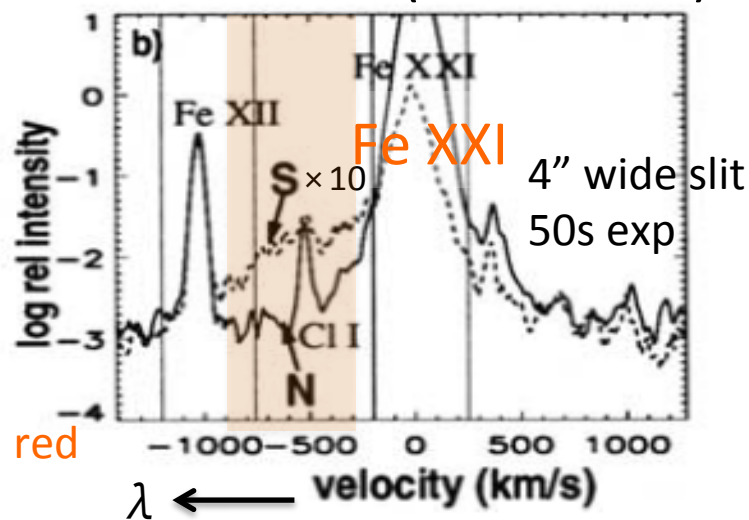
Wang+2007 (GOES M2.5)



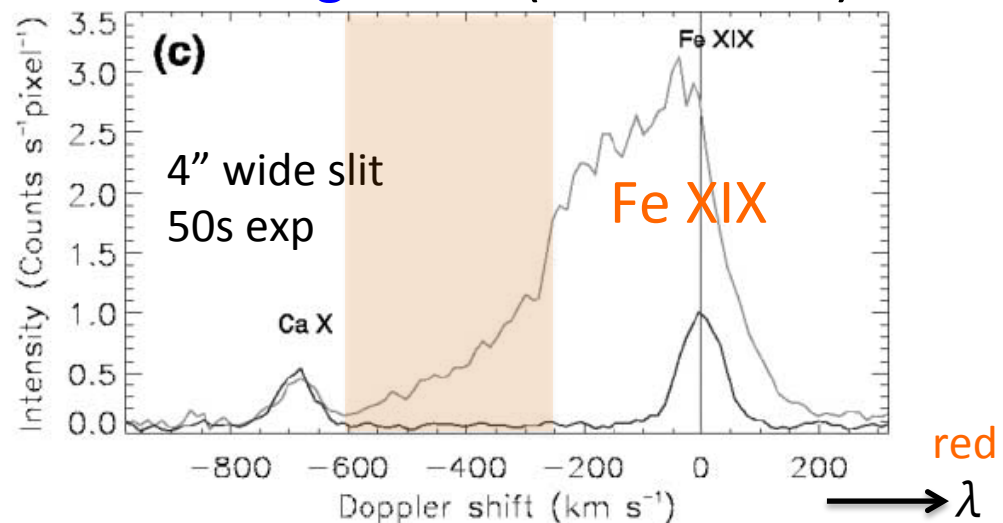
Reported EUV Observations of Reconnection Outflows

- A few cases have only been reported on the spectrum of reconnection outflow. **A dark structure in general.**
 - SOHO/SUMER: Innes+2003 (X1.5) Fe XXI } No scanning observations
 - Wang+2007 (M2.5) Fe XIX }
 - Hinode/EIS: Hara+2011 (B9.5) Fe XXIV, Fe XXIII, Ca XVII
 - Imada+2013 (X1.7) Fe XXIV

Innes+2003 (GOES X1.5)



Wang+2007 (GOES M2.5)



Reported EUV Observations of Reconnection Outflows

- A few cases have only been reported on the spectrum of reconnection outflow. **A dark structure in general.**

– SOHO/SUMER: Innes+2003 (X1.5) Fe XXI

Wang+2007 (M2.5) Fe XIX

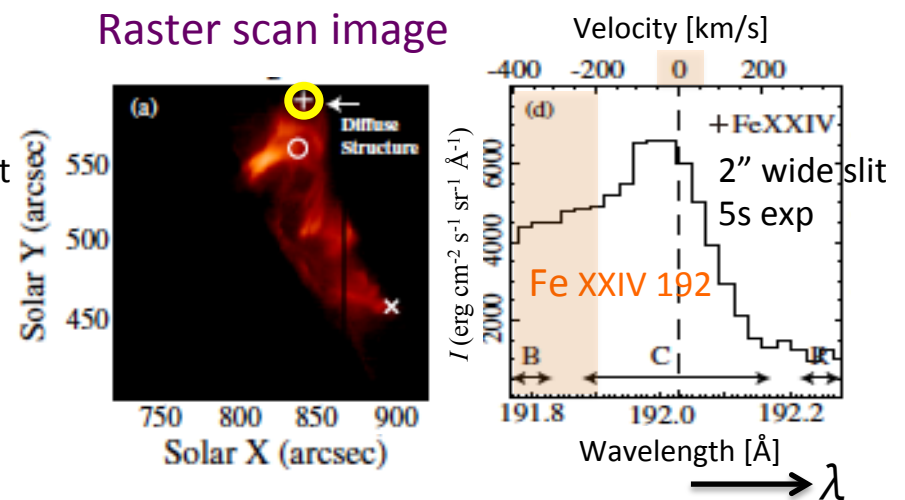
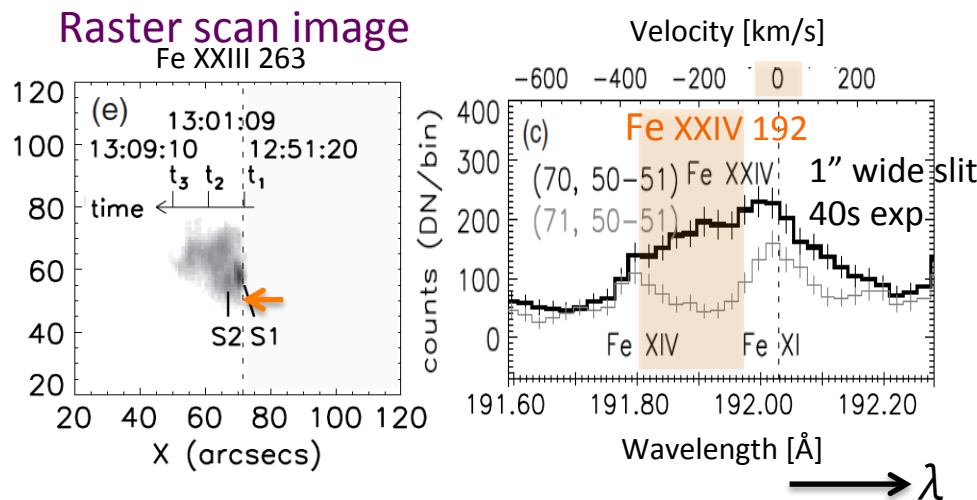
– Hinode/EIS: Hara+2011 (B9.5) Fe XXIV, Fe XXIII, Ca XVII

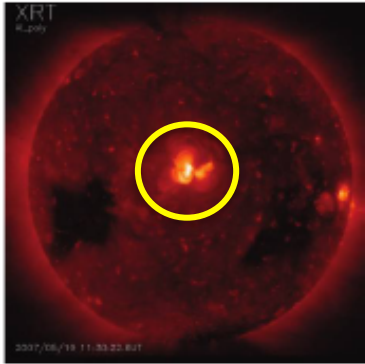
with scanning observations

Imada+2013 (X1.7) Fe XXIV

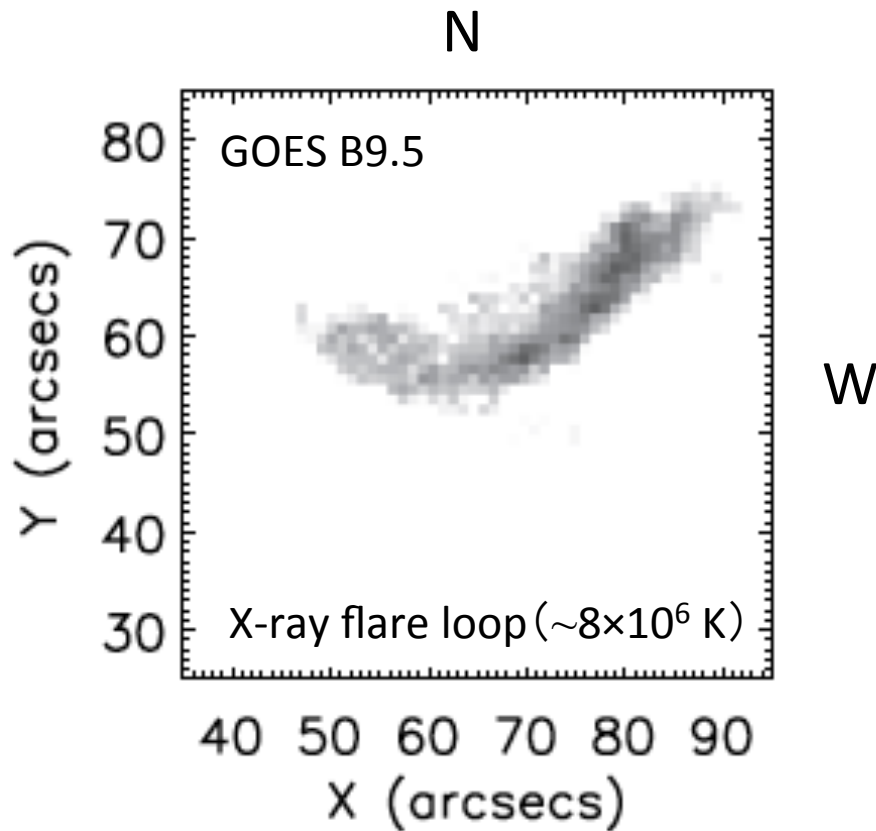
Hara+2011 (GOES B9.5)

Imada+2013 (GOES X1.7)

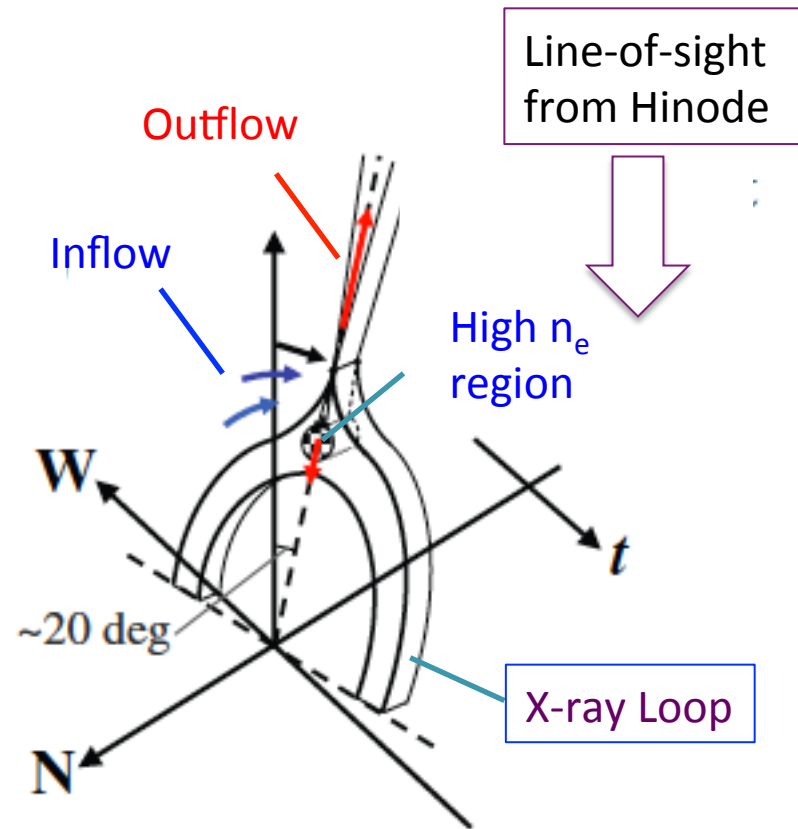


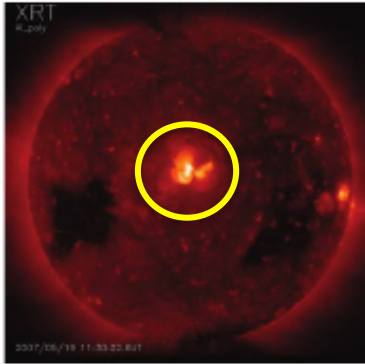


Magnetic Reconnection in an eruptive event



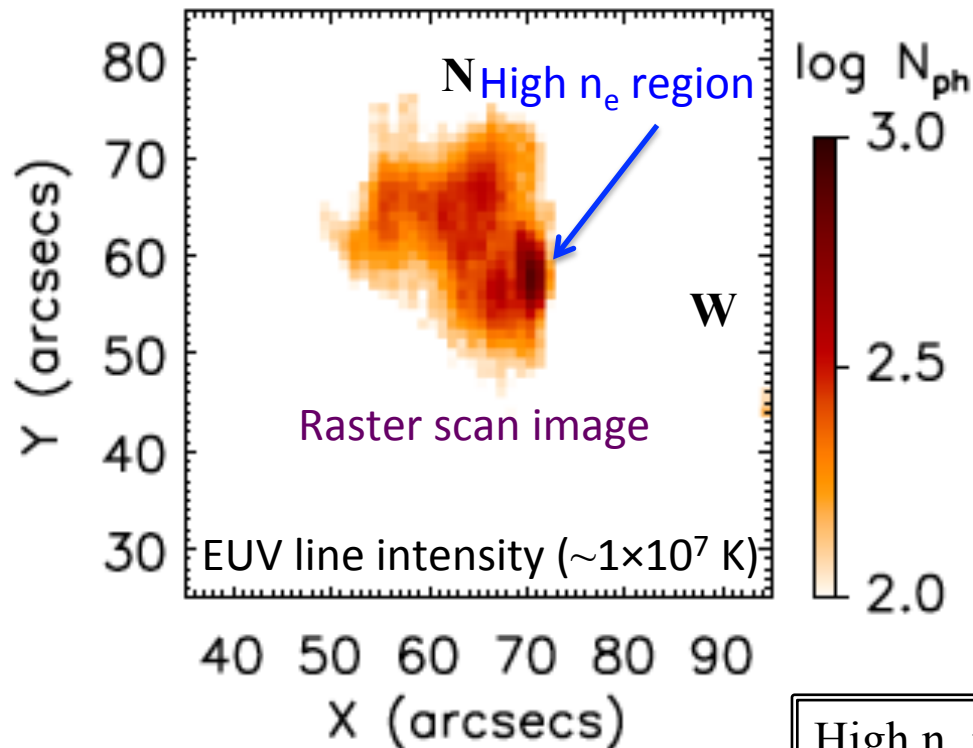
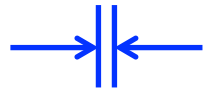
1 arcsec = ~ 700 km on the Sun



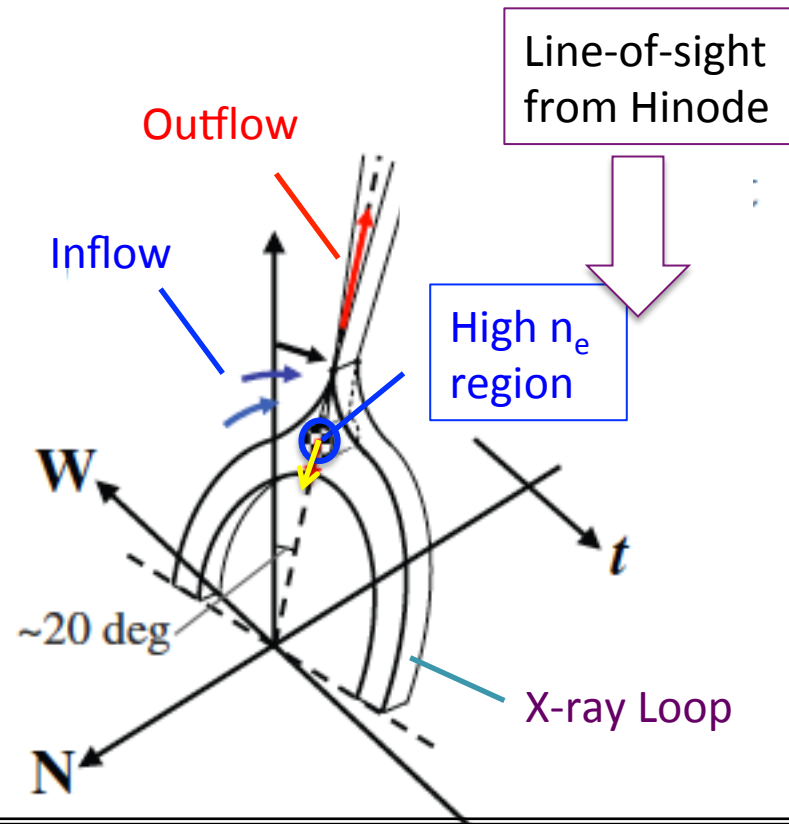


Magnetic Reconnection in an eruptive event

Duration of impulsive phase



1 arcsec = ~ 700 km on the Sun

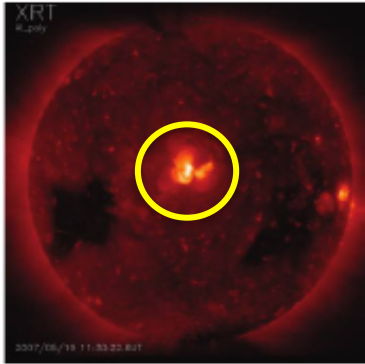


High n_e region:

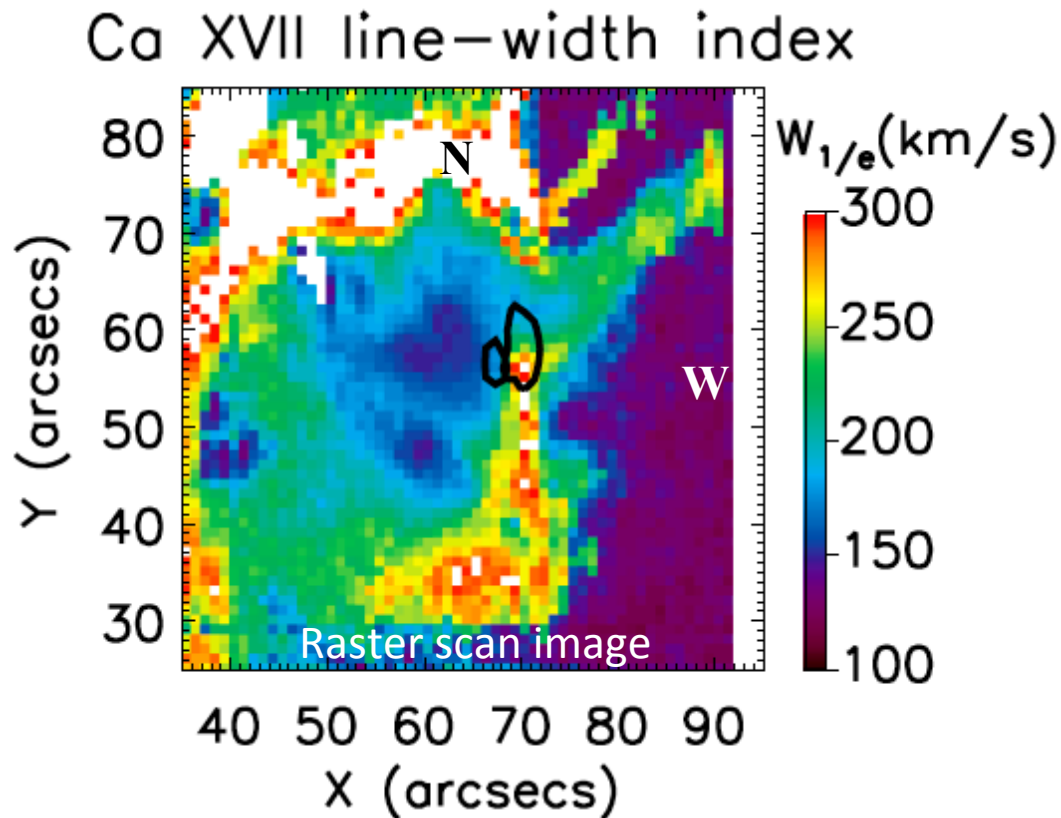
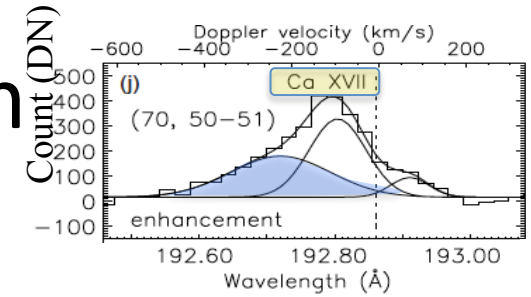
$T_e = 12$ MK [Fe XXIV/Fe XXIII, RHESSI continuum]

$T_i = 50$ MK (or $V_{NT} = 100$ km/s) [Fe XXIII line width]

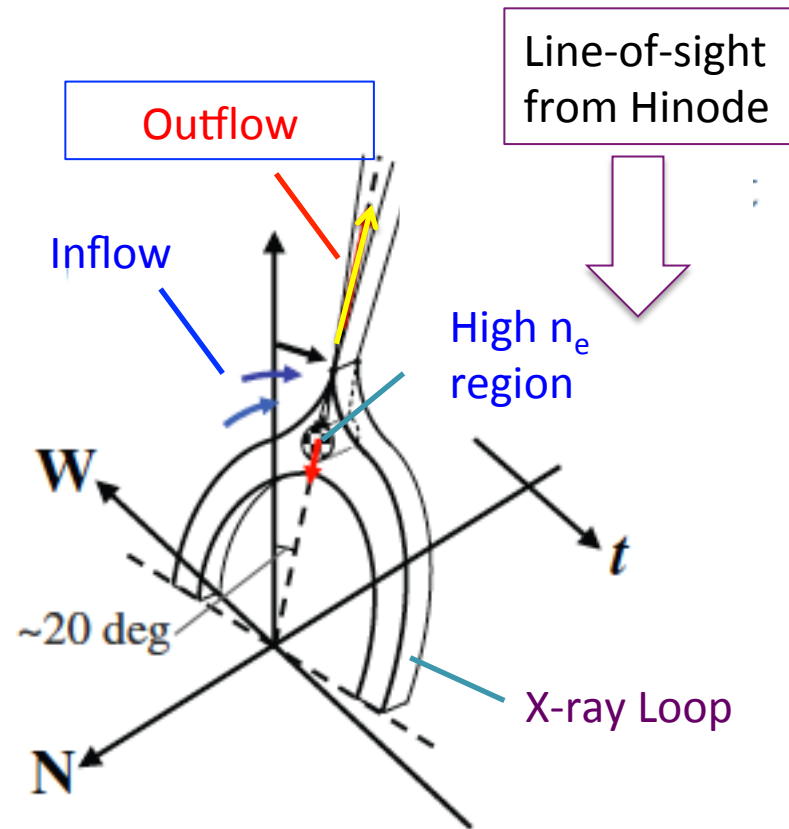
$V_D = 30$ km/s (downward)



Magnetic Reconnection in an eruptive event

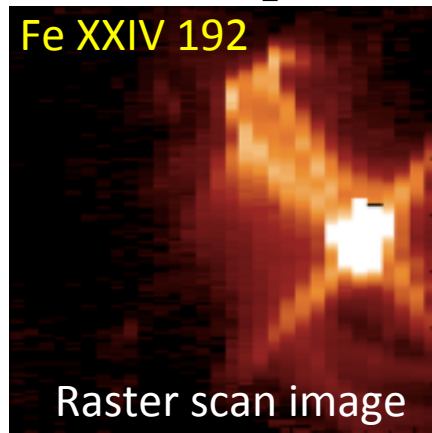


1 arcsec = ~700 km on the Sun



Outflow speed: $V_D = 200 - 400$ km/s

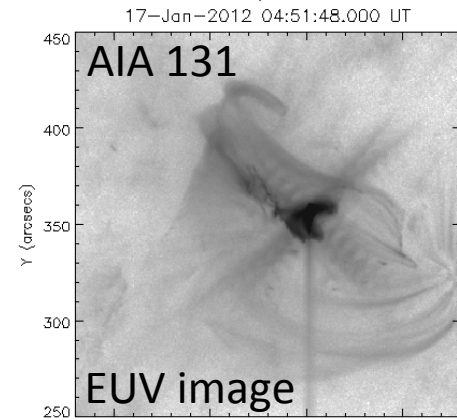
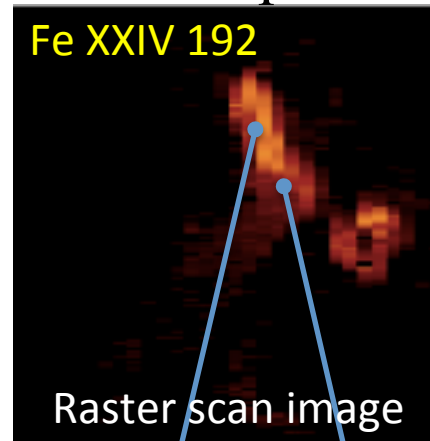
Slow component



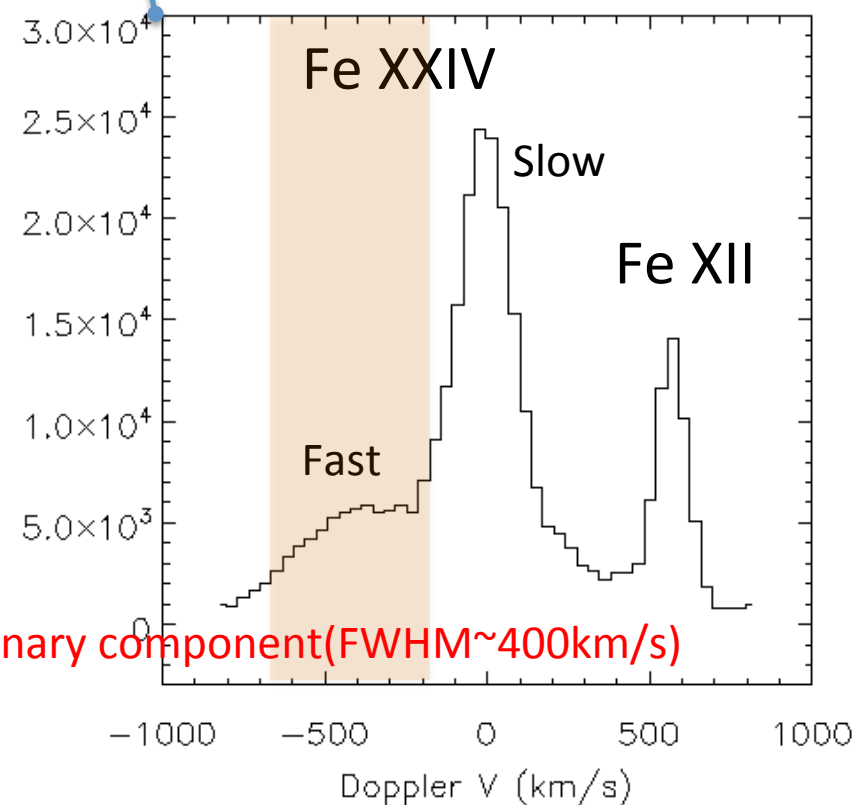
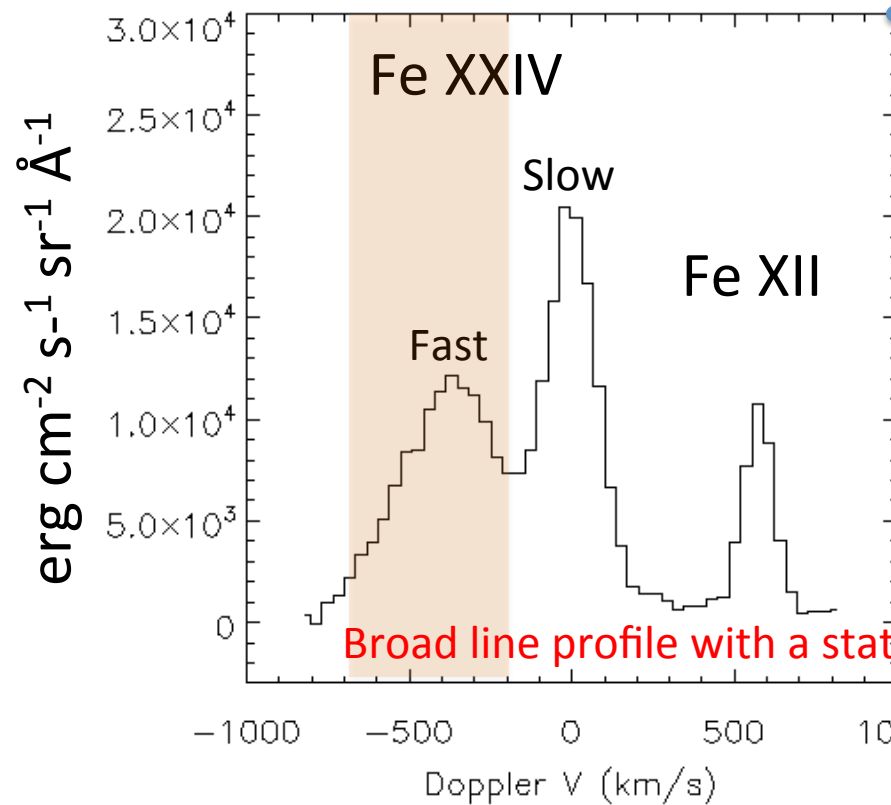
GOES M1.0

20120117 04:52:27

Fast component ($|V| > 200$ km/s)

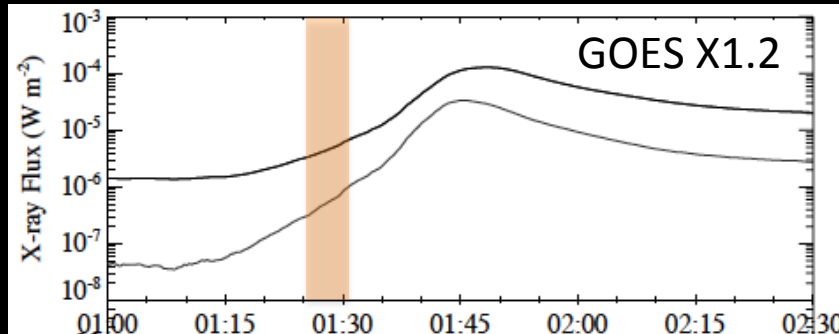


20120117 04:52:06



Broad line profile with a stationary component (FWHM ~ 400 km/s)

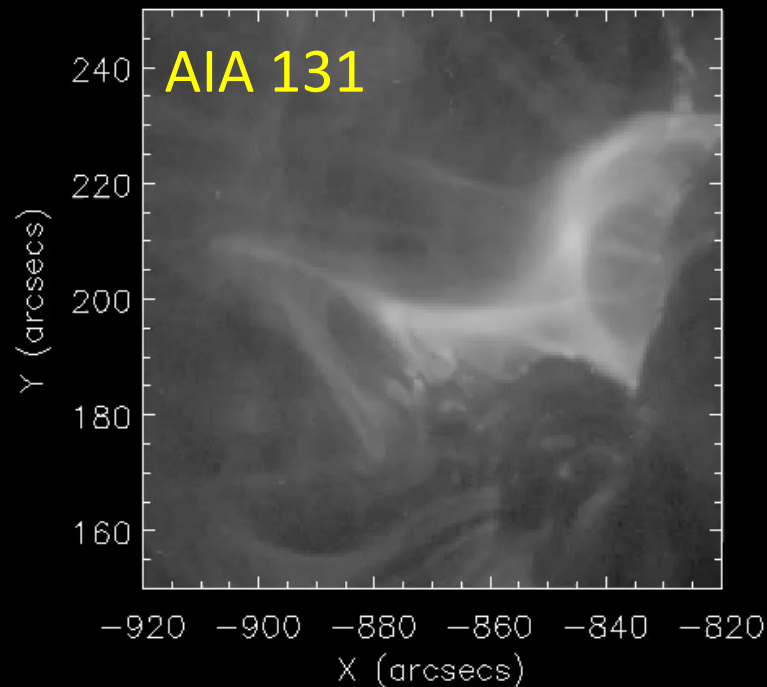
Dynamics in an EIS sparse raster



- Many changes are going on during a single EIS raster observation.

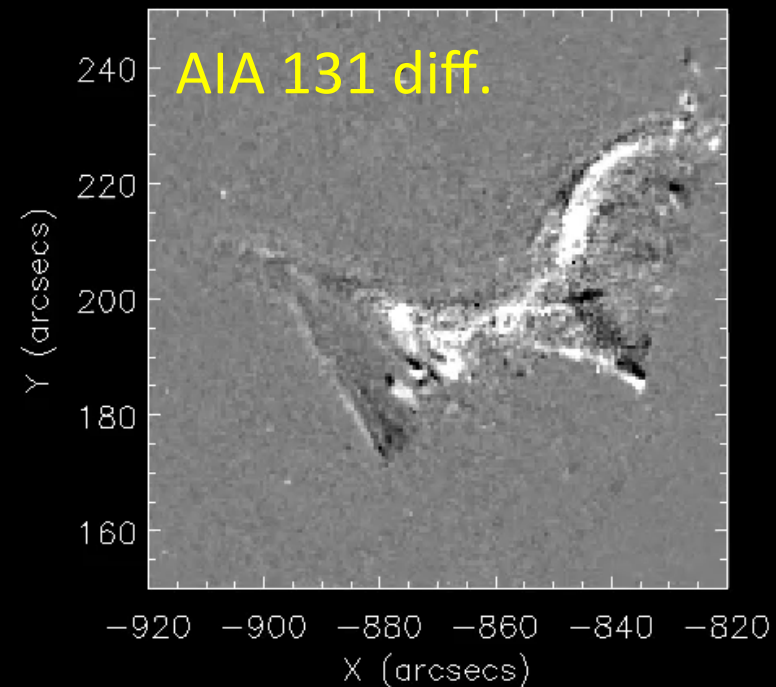
SDO/AIA 131

2013-05-15 01:24:56



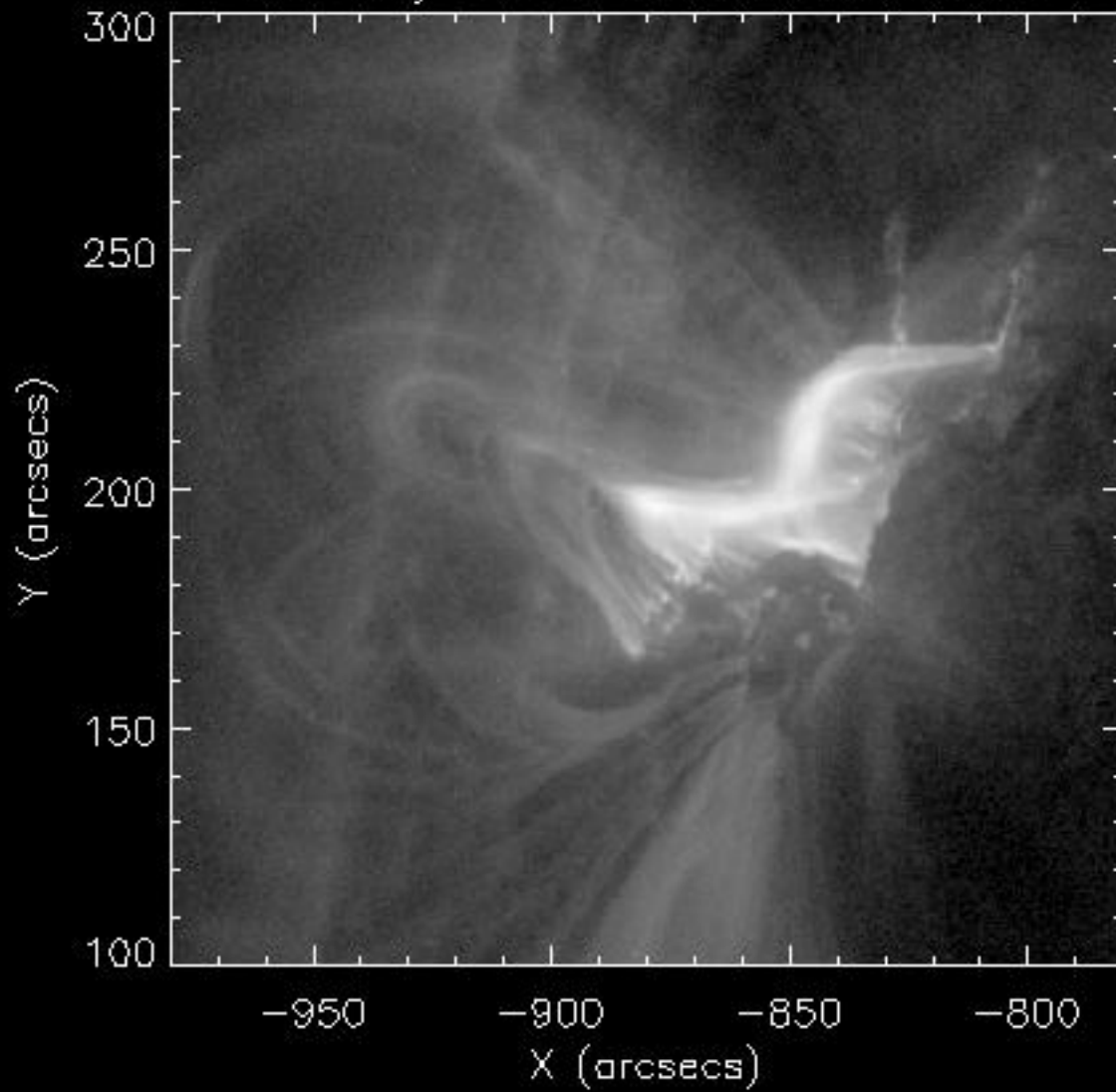
SDO/AIA 131

2013-05-15 01:24:56



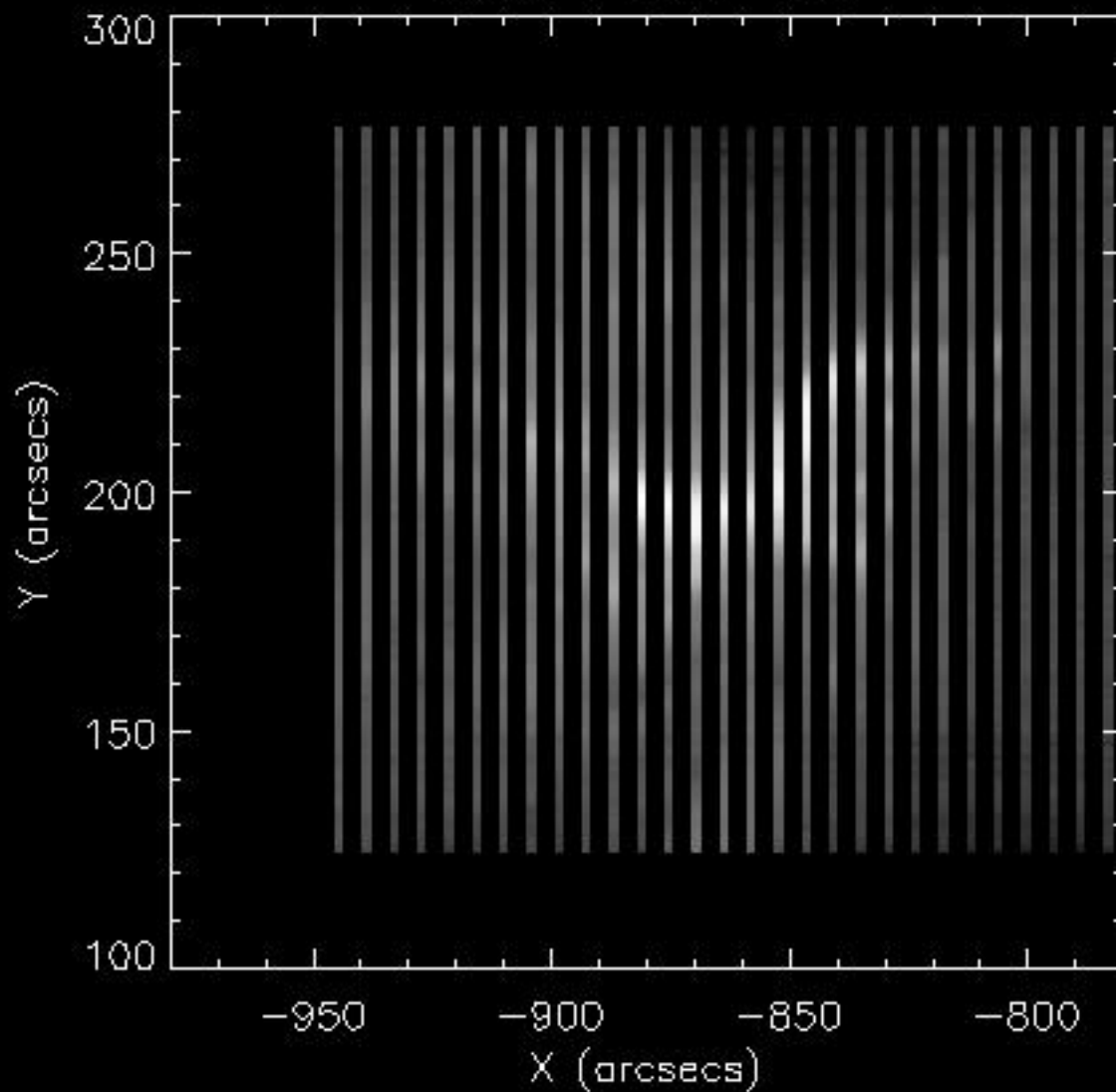
AIA 131

15-May-2013 01:28:56.620 UT



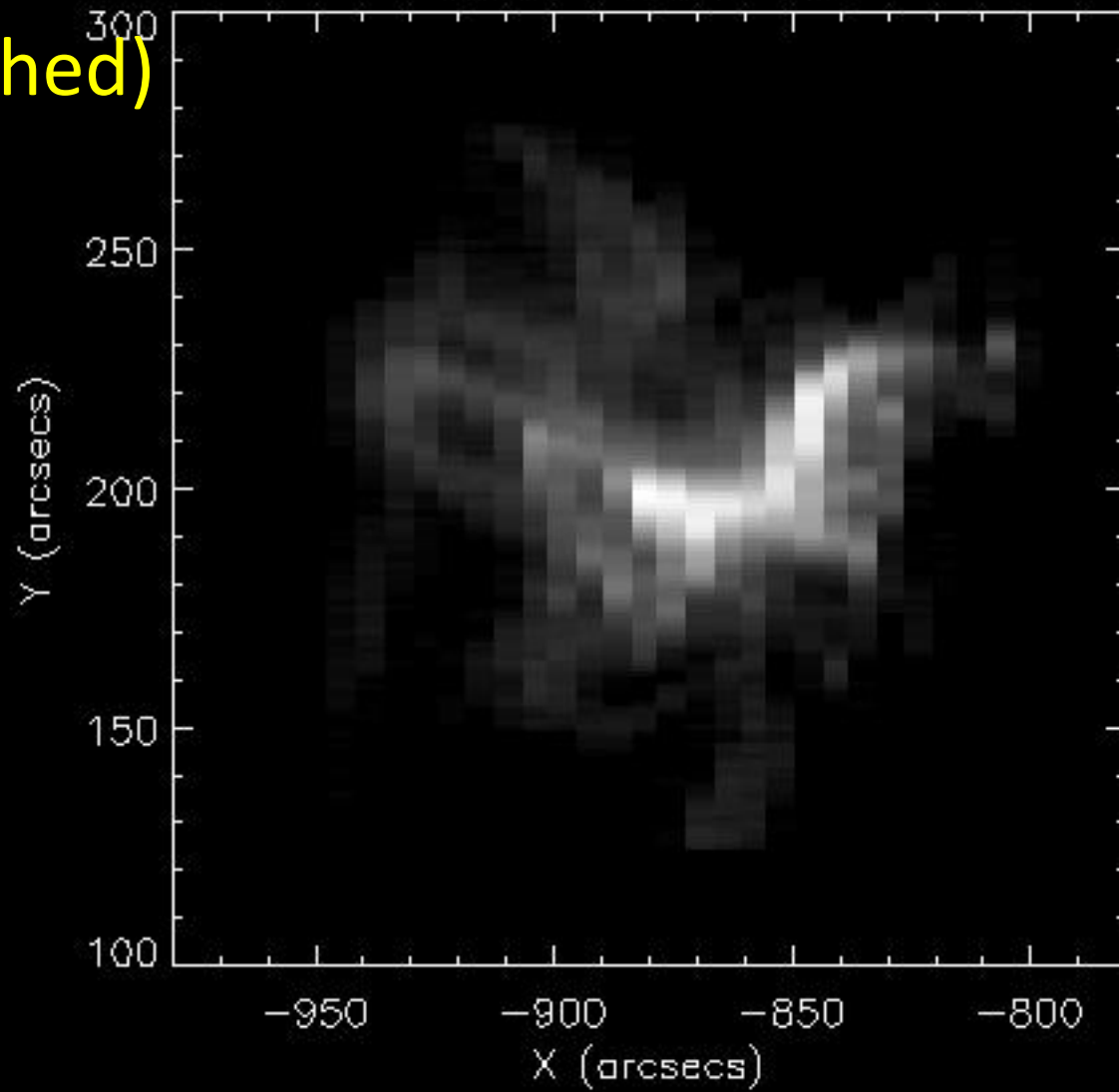
EIS Fe XXIV 192

EIS: Fe XXIV 192

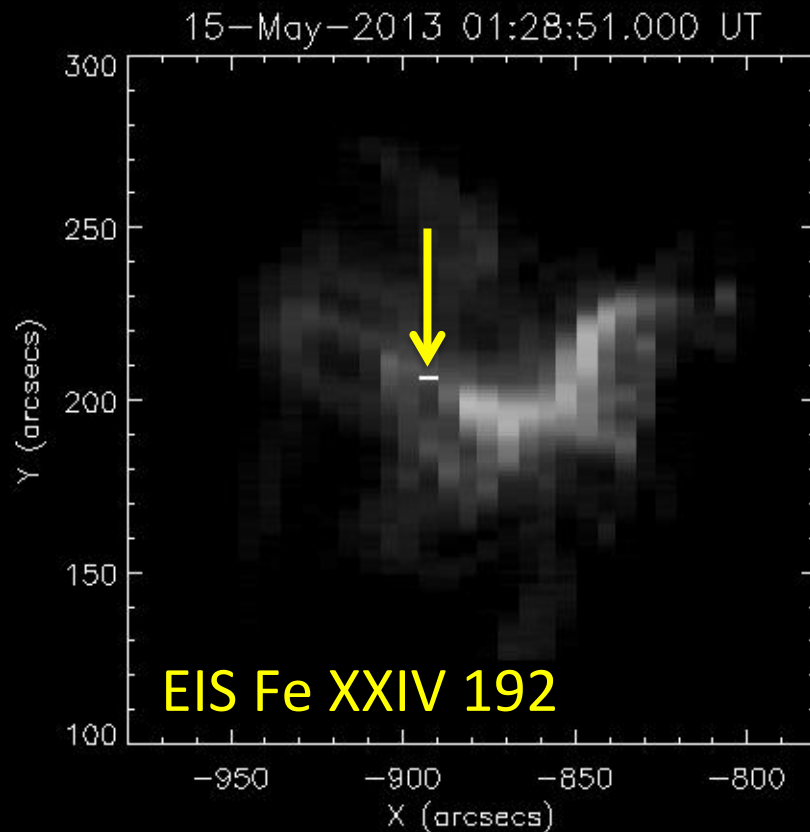


EIS Fe XXIV 192
(smoothed)

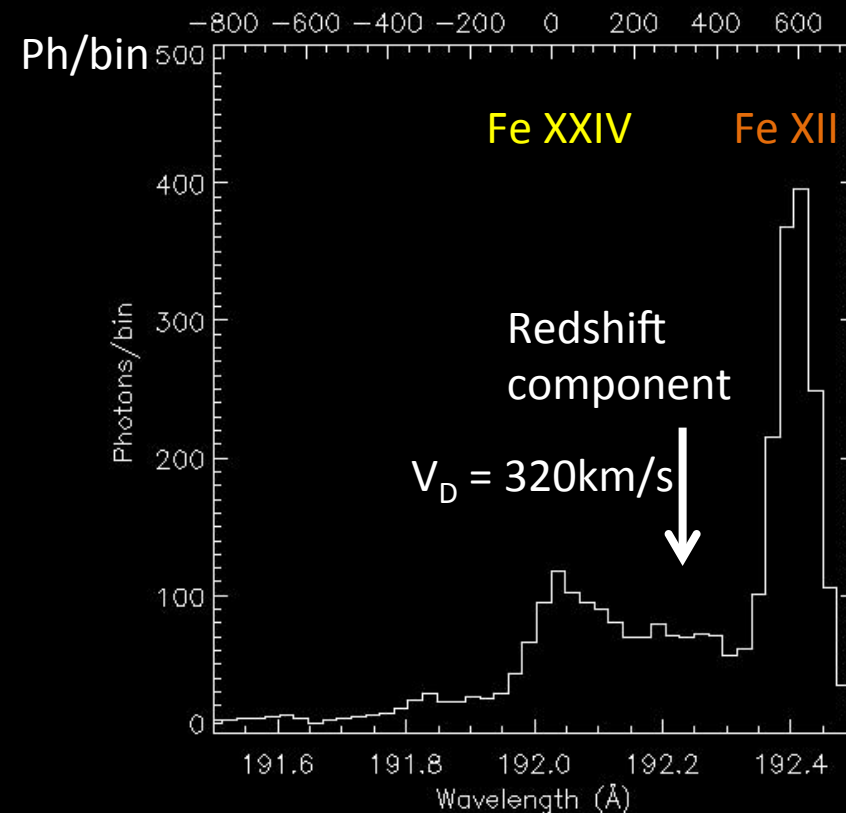
EIS: Fe XXIV 192



Spectrum in the thin structure above the cusp



Doppler Velocity V_D (km/s)



Broad profile with a stationary component

Shifted component: FWHM=400km/s

$V_{NT} = 230 \text{ km/s}$ ($T_i=1.0E7 \text{ K}$) or $T_i = 2.0E8 \text{ K}$

$$W_{\text{obs}} = \sqrt{W_I^2 + 4 \ln 2 \left(\frac{2kT_i}{M_i} + V_{NT}^2 \right)} \equiv \sqrt{W_I^2 + W^2}$$

MR: gain from *Hinode*

Recent EUV spectrograph observations have revealed:

Reconnection Inflow:

Speed: $V_D = 3 - 20$ km/s

- ❖ **Disappear** after entering reconnection region due to heating

$$M_{A, \text{inflow}} \sim 0.01 - 0.1$$

Slow & Fast Shock:

- ❖ Presence suggested from thermal parameters

$$\begin{aligned} T_{e, \text{outflow}}/T_{e, \text{inflow}}, \quad n_{e, \text{outflow}}/n_{e, \text{inflow}} \\ T_{e, \text{blob}}/T_{e, \text{outflow}}, \quad n_{e, \text{blob}}/n_{e, \text{outflow}} \end{aligned}$$

- ❖ An example: $V_{\text{outflow}}/V_{\text{fast}} > \sim 1.2$

Reconnection outflow/plasmoid:

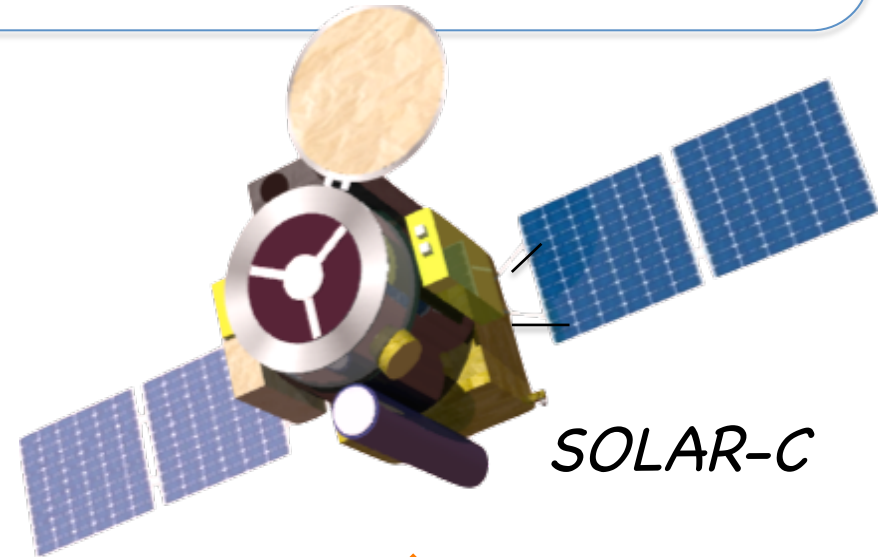
Speed: $V_D = 200 - 500$ km/s

some $V \sim V_A$

- ❖ **Dark structure in general**
- ❖ **Broad line profile (turbulence)**
- ❖ **with stationary component**
- ❖ **Bloppy structure, 3D geometry**
- ❖ An example: $V_{\text{outflow}}/V_{\text{fast}} > \sim 1.2$

Improved observations:

~30sec integration is required for pixel-by-pixel investigation using the current instrumentation in *Hinode*.



Further sensitivity for more rapid and pixel-by-pixel analysis

Summary

- From vector B measurements by Hinode and MHD simulations, some promising models for solar flare are appearing. Observations of chromospheric structures and B are crucial.
- Atmospheric response to the accelerated electrons in solar flares has been investigated from high-resolution imaging and TR-corona spectroscopy.
- Flow structures near the site of magnetic reconnection have been mapped in the EUV spectroscopy, and the presence of temperature structure in the current sheet may be becoming visible.